Bioorganic Chemistry 84 (2019) 418–433

Contents lists available at ScienceDirect

Bioorganic Chemistry

journal homepage: www.elsevier.com/locate/bioorg

N-Alkyl-1,5-dideoxy-1,5-imino-L-fucitols as fucosidase inhibitors: Synthesis, molecular modelling and activity against cancer cell lines

Jian Zhou[a], Arvind Negi[b], Styliana I. Mirallai[b], Rolf Warta[c], Christel Herold-Mende[c], Michael P. Carty[d], Xin-Shan Ye[e], Paul V. Murphy[b,*]

[a] School of Chemistry and Chemical Biology, University College Dublin, Dublin 4, D04 V1W8, Ireland
[b] School of Chemistry, National University of Ireland Galway, University Road, Galway H91 TK33, Ireland
[c] Division of Experimental Neurosurgery, Department of Neurosurgery, University of Heidelberg, Im Neuenheimer Feld 400, 69120 Heidelberg, Germany
[d] School of Natural Sciences, Biochemistry and Centre for Chromosome Biology, National University of Ireland Galway, University Road, H91 TK33 Galway, Ireland
[e] State Key Laboratory of Natural and Biomimetic Drugs and School of Pharmaceutical Sciences, Peking University, Xue Yuan Road No. 38, Beijing 100191, China

ARTICLE INFO

Keywords:
1-Deoxyfuconojirimycin
N-alkylation
Iminosugar
Fucosidase
Homology modelling
Anti-cancer activity

ABSTRACT

1,5-Dideoxy-1,5-imino-L-fucitol (1-deoxyfuconojirimycin, DFJ) is an iminosugar that inhibits fucosidases. Herein, *N*-alkyl DFJs have been synthesised and tested against the α-fucosidases of *T. maritima* (bacterial origin) and *B. taurus* (bovine origin). The *N*-alkyl derivatives were inactive against the bacterial fucosidase, while inhibiting the bovine enzyme. Docking of inhibitors to homology models, generated for the bovine and human fucosidases, was carried out. *N*-Decyl-DFJ was toxic to cancer cell lines and was more potent than the other *N*-alkyl DFJs studied.

1. Introduction

Iminosugars and their derivatives are inhibitors of enzymes of medicinal interest. These include glycosidases, glycosyltransferases [1,2], glycogen phosphorylases [3], nucleoside-processing enzymes [4], a sugar nucleotide mutase [5,6], metalloproteinases [7] and others [8]. Iminosugars inhibit glycosidases, due to their ability to bind at the active sites of these enzymes [9–11]. The range of enzymes inhibited by iminosugars indicates they have promise as new medicines for diseases such as diabetes, viral infections or lysosomal storage disorders [12] α-Fucosidase is involved in the removal of non-reducing terminal L-fucose residues that are connected to oligosaccharides via α-1,2; α-1,3; α-1,4 or α-1,6-linkages. L-Fucose (**1**) is found on glycans that participate in cell–cell interactions and cell migration. These events are connected to physiological and pathological processes such as fertilization, embryogenesis, lymphocyte trafficking, immune responses, and cancer metastasis [13–15]. A variety of physiological and pathological events are associated with fucose containing glycoconjugates. For instance, an aberrant distribution of α-fucosidase has been reported as being relevant to inflammation [16], cancer [17], and cystic fibrosis [18]. These enzymes have been recognized as diagnostic markers for the early detection of colorectal [19] and hepatocellular cancers, and this is due to the presence of α-fucosidase in patient serums. α-Fucosidase inhibitors may be used to study their functions and could form the basis of developing therapeutic agents [20]. Fuconojirimycins **3**, **4** and the 1-deoxy analogue **2** (DFJ) are key inhibitors of α-L-fucosidases. Other compounds assessed for their fucosidase inhibitory properties are also shown in Fig. 1 with their reported K_i values.

In recent years, *N*-alkylated iminosugars have shown improved *in vivo* and *in vitro* activities, mainly due to their improved lipophilicity, which may facilitate their crossing of the plasma membrane into cells [23–25]. In some cases, the appended alkyl groups are involved in hydrophobic interactions in the hydrophobic pocket of the target proteins. *N*-Butyl-1-deoxynojirimycin (zavesca®) has been approved for Gaucher disease and *N*-hydroxyethyl-DNJ (glyset®) is used for type-II diabetes associated complications [26]. Also, *N*-alkyl DNJs [27,28] such as zavesca®, *N*-nonyl-DNJ and **5a-c** [29] (shown in Fig. 2) act as highly potent pharmacological chaperones for the potential treatment of Gaucher [30] and Pompe [31] diseases by 'rescuing' mutant enzymes. Kelly et al. [32] and Overkleeft et al. [33] have shown that additional attachment of a large lipophilic substituent (such as the adamantyl group) (see **5d-e** in Fig. 2) increases the interaction with the glucocerebrosidase involved in lysosomal glycosphingolipid processing.

A number of *N*-alkyl DFJ derivatives have been synthesised pre-

* Corresponding author.
E-mail address: paul.v.murphy@nuigalway.ie (P.V. Murphy).

https://doi.org/10.1016/j.bioorg.2018.12.003
Received 9 October 2018; Received in revised form 23 November 2018; Accepted 3 December 2018
Available online 04 December 2018
0045-2068/

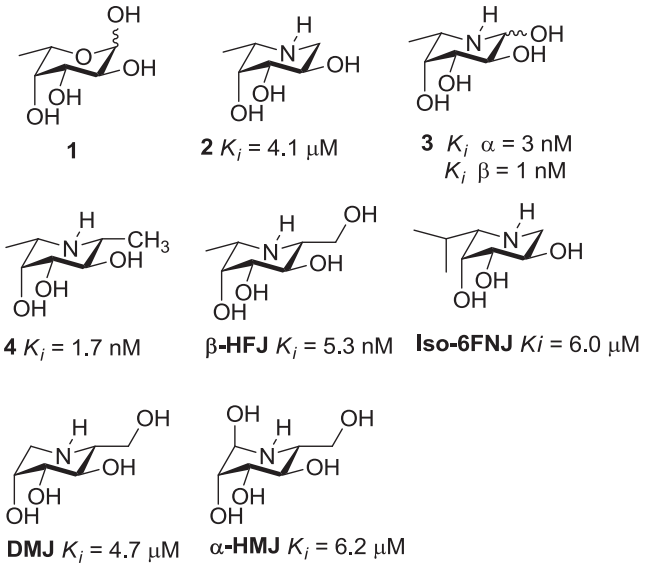

Fig. 1. Various fucosidase inhibitors: L-fuconojirimycin **3** & **4**) [21]; natural or semi-synthetic inhibitors contains 1-deoxyfuconojirimycin (**DFJ**), β-hydroxymethyl 1-deoxyfuconojirimycin (**β-HFJ**), 1-deoxymannojirimycin (**DMJ**), mannojirimycin (**α-HMJ**) [20,22].

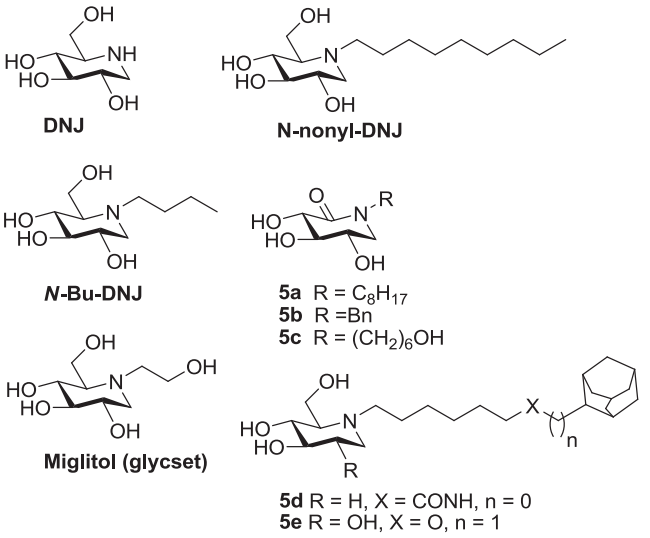

Fig. 2. Bioactive *N*-alkylated iminosugars.

viously. This includes an N-(aminopropyl) derivative prepared by Hung's group which had an IC_{50} of 70 nM as an inhibitor of the fucosidase from *T. maritima* [34]. Some *N*-alkyl DFJ derivatives have been evaluated against fucosyl transferases [35]. *N*-Methylated-DFJ showed weak anti-HIV activity and no cytotoxicity in a study where various glycosidase inhibitors were screened [36]. Conformationally constrained *N*-alkyl DFJ derivatives were inhibitors of bovine epididymis α-L-fucosidase [37]. An analogue of castanospermine with the L-fuco configuration and its fucosidase activity was described by Paulsen and co-workers [38].

Herein, the synthesis of new *N*-alkylated-1-deoxyfuconojirimycins and their testing against α-fucosidases and cancer cell lines has been carried out. Molecular modelling has been used to generate hypotheses about their modes of binding. *N*-Decyl-1-deoxyfuconojirimycin (*N*-decyl-DFJ) was found to be toxic against various cancer cell lines.

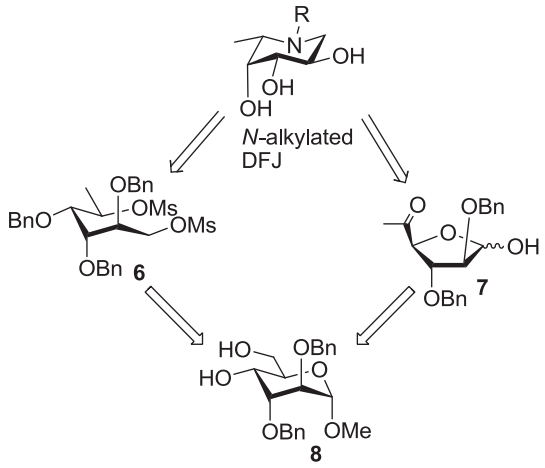

Scheme 1. Summary of the synthesis.

2. Results and discussion

2.1. Chemistry

The synthetic work investigated herein is summarized in Scheme 1. The attempted preparation of the *N*-alkylated DFJ derivatives was investigated initially from the altrose derivative **7** prepared from **8** as previously described [39,40]. However, synthesis from the Fleet bis-mesylate **6** [41] was ultimately the more successful route.

Compound **7**, which adopted a furanose structure was a mixture of anomers (α:β = 2:1). A double reductive amination reaction from **7** was initially investigated (Scheme 2) with a view to generating the required benzylated DFJ derivative [42,43]. *N*-Butyl amine was hence reacted with **7** in the presence of $NaBH_3CN$ and acetic acid in methanol at room temperature. The NMR analysis of the product mixture indicated formation of an inseparable mixture of 1,6-dideoxyaltronojirimycin (DAJ) derivative **9** and DFJ derivative **10** (ratio ~1:1, 79%). Instead, $NaBH(OAc)_3$ at various temperatures (−60 to −10 °C) was tried but a mixture of stereoisomers was still obtained [43]. The same approach using *N*-octylamine had a similar outcome. When benzyl amine was used, the epimers **9** (R = Bn) and **10** (R = Bn) could be separated and they were isolated in approximate equal amounts (36% for **9** and 40% for **10**). It was possible to improve the stereoselectivity of the reductive amination reaction by using a chiral amine [44,45]. When (*R*)-1-phenylethanamine was used, a single isomer **11** was obtained in good yield (85%). However, NMR experiments showed that **11** had an altrose configuration with its ring adopting the $^1C_4$ conformation; this was supported by coupling constants observed in the ^1H NMR spectrum ($J_{1a,2}$ = 8.6 Hz; $J_{1e,2}$ = 4.5 Hz). The reaction of the enantiomeric amine (*S*)-1-phenylethanamine was not stereoselective (Scheme 2).

The bis-mesylate **6** (Scheme 3) which Fleet [41] and his group used in a stereoselective synthesis of 1-deoxyfuconojirimycin was next prepared. The diol **13**[28] was converted to **6** and without chromatographic

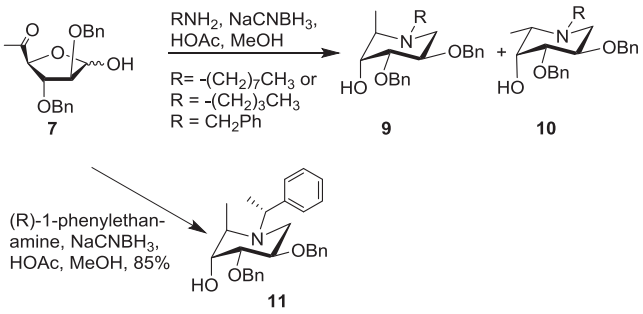

Scheme 2. Double reductive amination study from **7**.

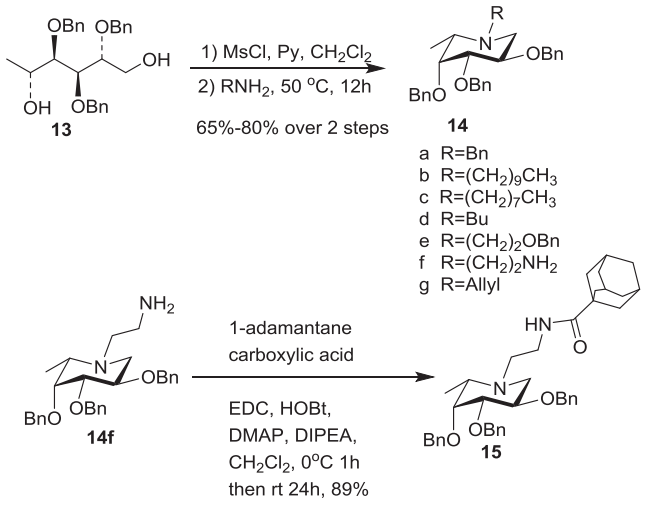

Scheme 3. The synthesis of **14** and **15**.

purification the freshly generated bis-mesylate was gently heated in the presence of various primary amines, giving *N*-alkyl DFJs. A number of *N*-substituted DFJs **14a-g** were thus obtained in 65–80% yield over 2 steps from the diol **13**. Adamantyl containing compounds have shown broad activities, including antiviral activity and for this reason were incorporated. Terminating the *N*-alkyl chains with a hydrophobic adamantyl group can lead to hydrophobic interactions with a target [46]. Thus, the *N*-ethylamine derivative **14f** was coupled with 1-adamantanecarboxylic acid in the presence of EDC and HOBt to give the adamantyl derivative **15** in 89% yield.

The benzyl protecting groups were removed from **14a–14e** and **15** by catalytic hydrogenation (Table 1, Scheme 4). The deprotection was first validated by the reaction of **14e** with Pd-C in the presence of hydrogen in THF-H_2O-HOAc (4:2:1) and this gave **16** in 78% yield after ion-exchange chromatography [47]. When **14a** was reacted in the same way then compound **22** was isolated. This is explained by the formation of DFJ **2** after removal of all the benzyl groups from **14a**. The DFJ **2** then reacted with traces of tetrahydrofuran-2-ol (or 4-hydroxybutanal) which could be formed from dihydrofuran (DHF) present in THF. The reaction of **2** with 4-hydroxybutanal would give the iminium ion **21** which would be further reduced with hydrogen to give **22** [48]. When the solvent was changed to methanol instead of THF then only **2** was obtained from **14a**. The reaction of **14b-e** and **15** gave **16–20** (Table 1). The hydrogenation reaction of **9** (R = Bn) and **11** gave 1,6-dideoxyaltronojirimycin **5** (R = H) while reaction of **10** gave 1-deoxyfuconojirimycin **2**.

The NMR spectral data for **2** coincided with those reported previously for 1-deoxyfuconojirimycin [41,49]. Although the NMR data of

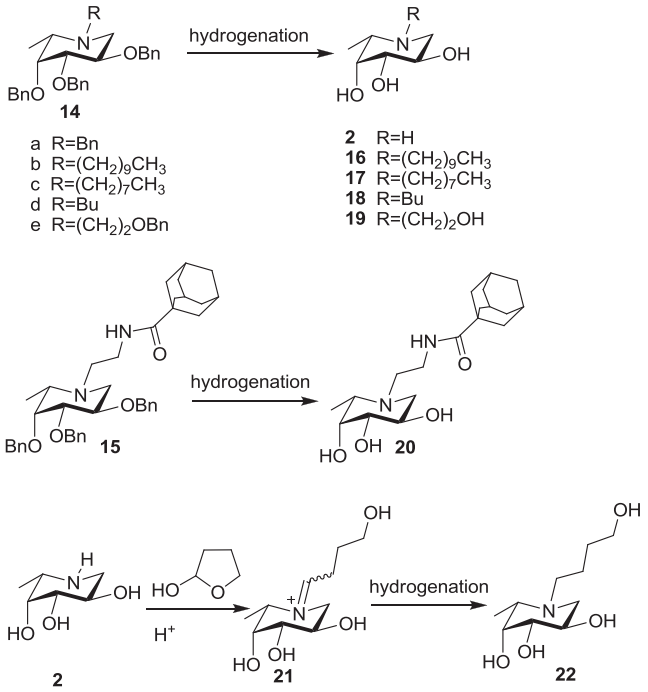

Scheme 4. Formation of DFJ **2** and derivatives.

compound **5** has not been reported previously, its specific rotation agreed with the earlier reported value: $[\alpha]_D^{20}$ 0.9 (*c* 0.55, MeOH) [lit. $[\alpha]_D^{20}$ 2 (*c* 1.1, MeOH)] [50,51].

2.2. Inhibition of fucosidases and structure activity relationship

The *N*-alkyl DFJs were tested as inhibitors of the fucosidase from *T. maritima* (bacterial origin) and *B. taurus* (bovine origin), and the IC_{50} values obtained are summarized in Table 2. The *T. maritima* enzyme shares 38% identity with its human counterpart and is speculated to have a role in modification of hemicelluloses [47]. The bovine derived fucosidase has been widely used in *N*-glycan, blood group oligosaccharide and glycolipid analysis. Only DFJ (**2**) showed moderate inhibition (IC_{50}, 8 μM) of the fucosidase from *T. maritima*. The active site of the fucosidase from *T. maritima* did not tolerate the presence of a butyl or hydroxybutyl group on the piperidine. Examination of the binding pose of L-fucose with the α-fucosidase of *T. maritima* in its co-crystal structure [52] indicated that the L-fucose is tightly enveloped by residues in the enzyme. These residues (see in Fig. 3) could prevent binding of *N*-substituted iminosugars assuming the fucopyranose mimetic **2** binds in a similar manner to L-fucopyranose.

Table 1
Formation of DFJ derivatives by catalytic hydrogenation.[a]

Entry	Reactant	Conditions[a]	Product	Isolated yield (%)[b]
1	**14a**	MeOH, HCl aq.	**2**	92
2	**14a**	THF, H_2O, HOAc (4:2:1)	**22**	85
3	**14b**	MeOH, HCl aq.	**16**	90
4	**14c**	MeOH, HCl aq.	**17**	85
5	**14d**	MeOH, HCl aq.	**18**	88
6	**14e**	THF, H_2O, HOAc (4:2:1)	**19**	78
7	**15**	MeOH, HCl aq.	**20**	83
8	**9**	MeOH, HCl aq.	**5**	93
9	**10**	MeOH, HCl aq.	**2**	89
10	**11**	MeOH, HCl aq.	**5**	83

[a] Pd-C, H_2, with various solvents and acids.
[b] After ion exchange chromatography.

Table 2
IC_{50} values (μM) and other parameters.

Compound	IC_{50} (fucosidase from *B. taurus*)	IC_{50} (fucosidase from *T. maritima*)	*LogP*[d]	LogD	For fucosidase from *B. taurus*	
					pIC_{50}	LipE[e]
2 (DFJ)	0.3 (0.4) [53]	8	−1.71	−2.23	6.52	8.75
17	25	*N. D.*[b]	1.723	1.02	4.60	3.57
16	2.5	*N. D.*	2.60	2.04	5.60	3.55
18	> 100	> 100	−0.04	−1.02	< 4	*N. A.*
19	27	*N. D.*	−2.13	−1.83	4.56	6.40
22	30	> 100	−0.07	1.05	4.52	3.47
20	90	*N.D.*	−1.25	−1.81	4.04	5.86
5	> 100	> 100	−1.71	−2.23	< 4	*N.A.*

[b] *N.D.* = not determined.
[d] Based on Labute et al. method calculated by CCG MOE2018.01.
[e] LipE = pIC_{50} - log D [55].

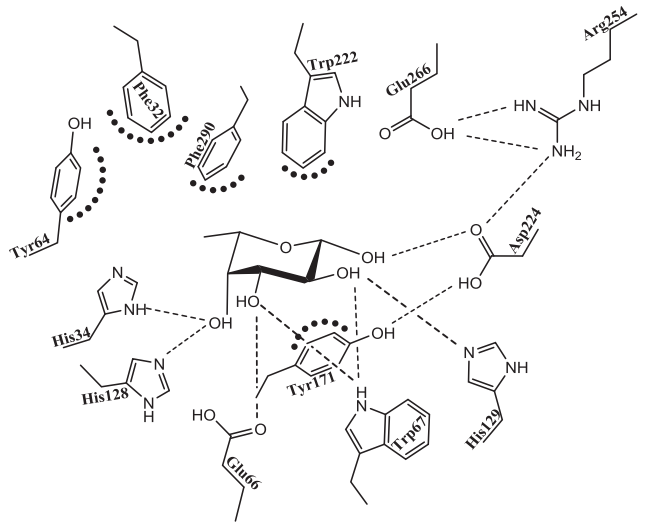

Fig. 3. The interactions between α-fucosidase from *T. maritima* and α-L-fucopyranose. H-bonds are shown as dashed lines, and van der Waals contacts are shown as bold dotted lines.

The *N*-butyl derivative **18** did not inhibit, at concentrations up to 100 μM, the fucosidase *B. taurus* from bovine kidney (Table 2), whereas the butanol derivative **22** had an IC_{50} of 30 μM. We determined an IC_{50} of 0.3 μM for **2** which agreed with a reported IC_{50} for **2** (0.4 μM) for the fucosidase from *B. taurus* [53]. However, lengthening the alkyl chain led to improved activity for as seen for *N*-decyl derivative **16** (IC_{50} = 2.5 μM). By comparing the aliphatic side chains of **16–18**, it can be concluded that having a longer alkyl group gives rise to improved inhibitory activity. Compound **20** which had an adamantyl group on the *N*-side chain was less potent with an IC_{50} of 90 μM. The *N*-ethanol derivative **19** showed IC_{50} value of 27 μM, similar to that of the *N*-butanol derivative The altronojirimycin derivative **5** (Table 1) did not show any inhibition towards the tested α-fucosidases.

In addition to the IC_{50} determination, some physiochemical parameters (LogP, LipE and logD) were calculated. In terms of oral administration, LogP values should be less than 5 according to Lipinski's rules of five, which most of the *N*-alkylated derivatives show [54]. LogP values between 2 and 3 are often considered optimal to achieve a compromise between permeability and first pass clearance, which is quite comprehensively shown by compound **16**. LipE is another parameter which links the potency (IC_{50}) and lipophilicity (logD) in an attempt to estimate drug-likeness of a particular structure. A satisfactory LipE value would indicate selectivity for the target of interest versus a generic hydrophobic environment [55]. A LipE measurement of 6 represents one-million-fold selectivity for the target versus a generic hydrophobic environment while a LipE of zero indicates no selectivity. Compounds **2** and **19** had values higher than 6.

2.3. Molecular modelling

Molecular modelling was used in order to hypothesise how the fuconojirimycin derivatives may interact with the fucosidases and to provide a basis for the development of more potent inhibitors. The 3D-coordinates for the fucosidase from *T. maritima* (PDB code: 2ZXD) were retrieved from Royal Collaboratory for Structural Bioinformatics Protein Data Bank (RCSB-PDB) [56]. The fucosidase of bovine origin was modelled using the α-L-fucosidase of *T. maritima* as a template. The sequence for the bovine fucosidase *B. taurus* was obtained from NCBI (National Center for Biotechnology Information). A BlastP search was then conducted which showed a number of possible templates for constructing the homology model (results from the BlastP search are provided in the supplementary information). Five templates were found

Table 3
Evaluation of the constructed homology models prepared from five available PDBs with identity ≥ 35% in their amino acid sequence. Qualitative structural measurements are provided in the form of Ramachandran plot, ERRAT plot, Verify-3D, ProA, Z-Score and superpose of homology model with their templates.

Models	Ramachandran Plot[a]				ERRAT Plot	Verify 3D	Superpose RMSD (Å)	ProSa Z-Score		
	% residue in favoured region	*% residue in additional allowed region*	*% residue in generously allowed region*	*% residue in* disallowed region			Template	Homology model	Template	$\Delta_{Z\text{-score}}$
1	85.1	7.3	0.6	0.9	84.57	80.65	1HL9_B (0.739)	−7.26	−9.87	0.26
2	84.5	13	1.5	0.9	86.74	89.25	2ZWY_A (1.174)	−7.47	−10.29	0.27
3	88.2	9.3	1.5	0.9	82.20	80.11	1HL9_A (1.050)	−6.96	−9.33	0.25
4	85.1	12.1	1.9	0.9	86.04	87.37	2WSP_A (0.926)	−7.69	−10.27	0.25
5	69.7	25.7	3.1	1.5	79.73	86.24	1ODU_A (1.89)	−6.75	−9.81	0.31

[a] Residues in Ramachandran plot are calculated as ~0.3 = 1.

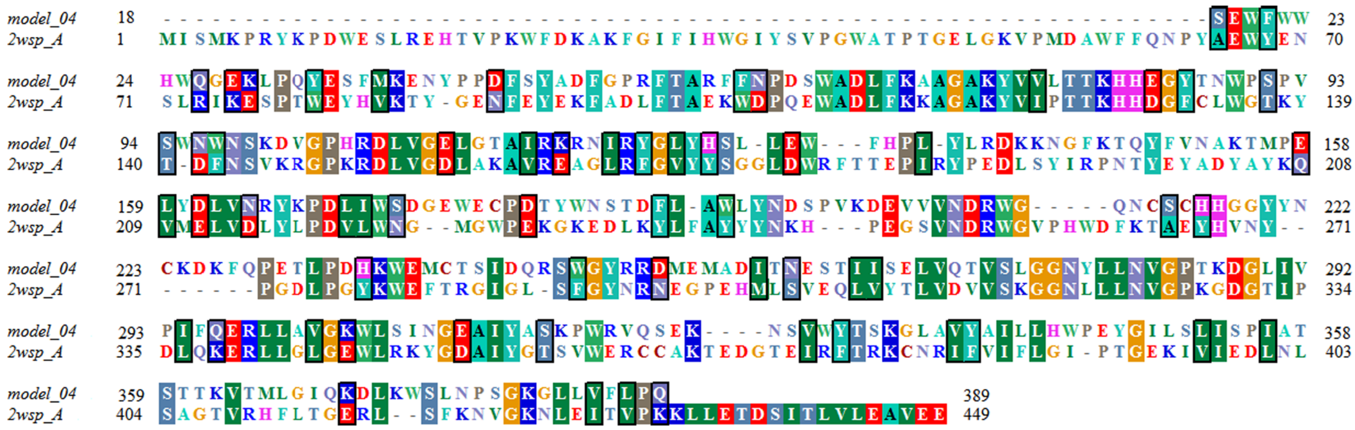

Fig. 4. The sequence alignment of model 4 with its template 2wsp_A showing evolutionary conserved residues.

with > 35% of residues matching, and the length of each template was ≥85% of that of the *B. taurus* input sequence and therefore homology models were built for each of these. These homology models were then evaluated based on their qualitative structural uniformity. Model-4 (Table 3) developed based on the template of a fucosyl hydrolase from a strain of *T. maritima* was selected based on the data presented in Table 3 for further molecular modelling studies. Three residues were found to be outliers in this model, and they were later were energy minimised. The plots obtained before and after minimisation are provided in the supplementary information. Comparing the pairwise sequence alignment of fucosidase of *B. taurus* with that from *T. maritima* showed the similarity of their structures (Fig. 4).

The docking of **2** with the crystal structure for the fucosidase from *T. maritima* was carried out and it suggested a H-bond acceptor/donor network, where hydroxyl groups of the iminosugar interacted with the side chain of Glu66 (1.97 Å), Trp67 (2.33 Å) and Asp224 (2.04 Å), as shown in Fig. 5A. The protonated nitrogen of the iminosugar had a H-bond donor interaction with the carboxyl group in the side chain of Asp224 (2.05 Å). The docking showed how closely the calculated binding mode of **2** resembles the already reported binding of iso-6FNJ in the crystal structure bound to the fucosidase from *T. maritima* (see Fig. 5B). Furthermore, the docking of **2** with the homology model of the *B. taurus* fucosidase indicated similar binding interactions to those seen for *T. maritima*. The hydroxyl groups of **2** had H-bond acceptor/donor interactions with Val77 (2.25 Å) and Asn282 (2.31 Å), while the protonated nitrogen was predicted to have H-bond donor interactions with Cys240 (2.45 Å), see in Fig. 5C. Also, a similar trend was noted after docking of **16** as its C-4 hydroxyl group was involved in a H-bond donor interaction with Cys240 (1.94 Å), while the protonated nitrogen had a H-bond donor interaction with Cys240 (1.92 Å). The nonane chain of **16** was placed by docking into a hydrophobic cavity constituted by aromatic residues (His82, Tyr126, Trp172) on one side while residues 281–283 and Trp248 were found on the other side of the domain. These are shown in Fig. 5D.

In order, to gain confidence regarding the reliability of the docked poses for **2** and **16**, they were selected for 100 ps molecular dynamics simulations (MD). The complex of **2** with the fucosidase of *T. maritima* showed stability after 10 picoseconds (ps) of the simulation (RMSD was consistently ~1.9 Å, Fig. 6A). The same protocol was applied on the docked complex of **2** with the fucosidase of *B. taurus*; the ligand-protein complex showed fluctuation in first 10 ps and then the RMSD maintained a stable value ~2.8 Å (Fig. 6B). The complex of **16** to fucosidase of *B. taurus* complex showed stability after 20 ps with an RMSD value of ~3.2 Å (Fig. 6C). The MD simulation demonstrated the docked ligand-protein complexes were stable and generated confidence that they form the basis of a reasonable hypothesis as to the nature of inhibitor binding [57].

To further evaluate molecules against human fucosidase, a reverse docking strategy was performed [58–61]. The consistency and suitability of docking placement methods (in MOE 2018.01) with respect to the activities of compounds were evaluated. Hence the 3D structure of human alpha fucosidase was next modelled using the same template which was used for fucosidase of *B. taurus* origin (2WSP_A). The quality of the human homology model generated (Fig. 7A) was evaluated using Verify 3D (88.81%) and Errat (88.86), Ramachandran plot (residues in most favoured regions (86.9%), residues in additional allowed regions (10.5%), residues in generously allowed regions (1.4%) residues in disallowed regions (1.1%,)) and ProSA Z-score (plots are available in *supporting information*). The residues Lys52, Phe184, His396 and Asp432 were found as outliers and are not in the active site (Fig. 7B)

The IC_{50}/K_D values (Table 4) for inhibitors (Fig. 8) of the human fucosidase (HuF) from the work of Ho et al. [62] were used to generate scatter plots (see Fig. 9). Trend lines were generated and R^2 values were determined; these showed an association between the docking placement method with respect to the inhibitory properties. The docking scores are shown in Table 4.

For this study, three different docking placement methods, available in MOE 2018.01, were investigated. Of the docking methods, the triangle matcher placement method performed better than the alpha triangle and alpha PMI placement methods. With this method there were coefficients of determination of 0.908 and 0.8731, which were higher than those of the other two methods (see Figs. 9 and 10).

The available enzyme inhibitory data from Ho et al. [34] for the two different enzymes were used to generate the plot in Fig. 11. These gave a trendline with an R^2 value of 0.7169. The R^2 values observed are sufficiently high to imply that the enzyme inhibitory properties for compounds are associated with binding to the specified active site cavity in the fucosidases [63].

The three docking methods all predicted that the *N*-propyl amine derivative **29** could have a different binding location within the active site (E-Score = −10.288) compared to other DFJ derivatives (Fig. 12).

In the docking of **18** (E-score = −5.613) and **22** (E-Score = −6.175) high E-scores were found, which are consistent with the lack of inhibition of the enzymes observed experimentally.

On the other hand, the *N*-butyl alcohol derivative **22** did show inhibitory activity (IC_{50} = 30 μM) towards the fucosidase of *B. taurus* and docking indicated this could be reasonably supported by the OH group of the butyl chain being involved in a hydrogen bonding interaction with the peptide backbone of Lys74 (2.97 Å) of this fucosidase (see Fig. 13).

The docking was also performed on human fucosidase (HuF) where binding of both the *N*-propylamine derivative **29** (E-score = −9.322) and *N*-decyl derivative **16** (E-score = −8.724) is predicted to occur (Fig. 14**A**). The difference between the binding score of **16** (E-score = −8.724) to HuF and to the fucosidase of *T. maritima* (E-score = −6.901) indicates it may be of interest to evaluate **16** for its inhibition of human fucosidase in due course.

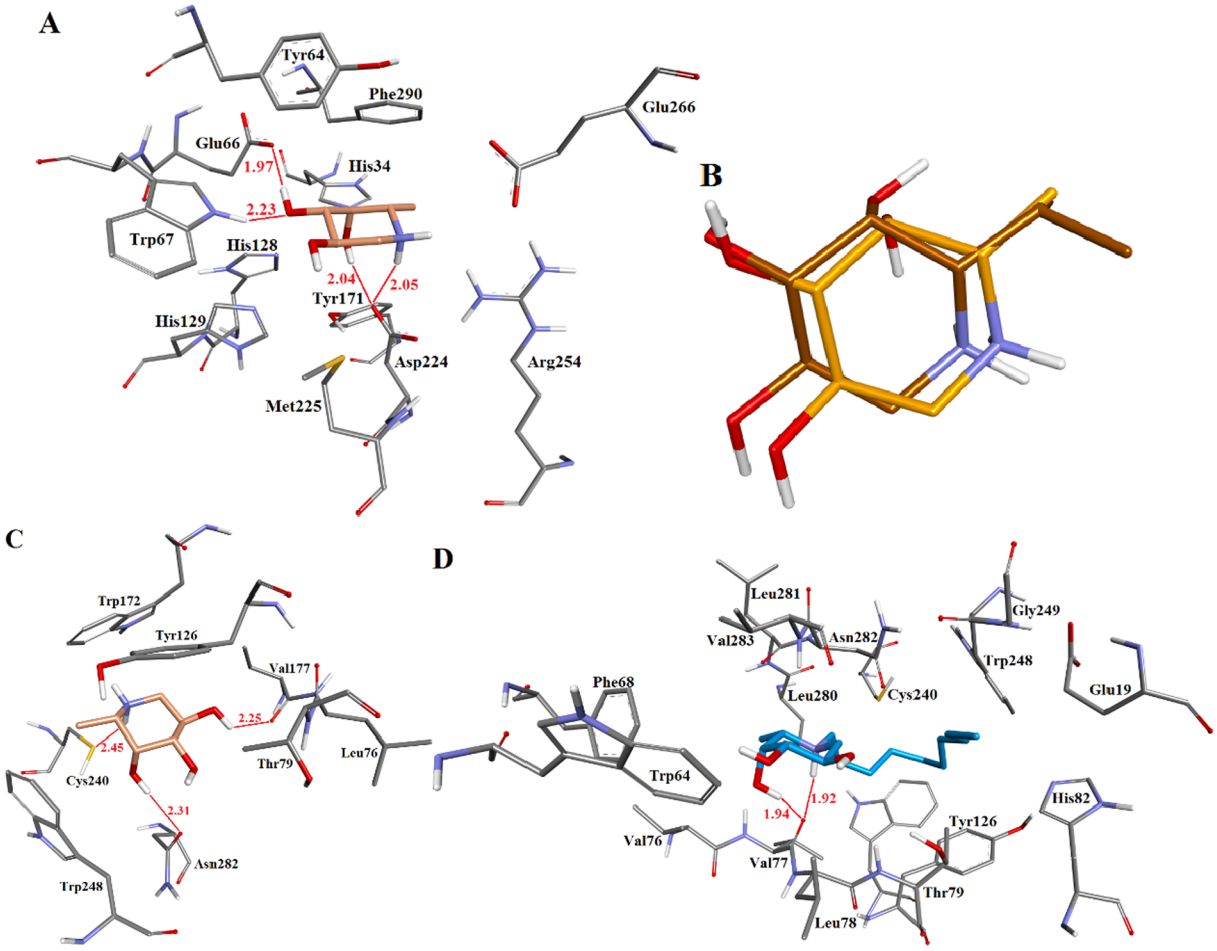

Fig. 5. (A) The docking pose of **2** (orange) with the fucosidase of *T. maritima*; (B) superpose of binding pose of **2** (orange) with co-crystallised ligand (brown) of 2WSP_A (model 4, Table 3); (C) docking pose of **2** with fucosidase of *B. taurus*; (D) docking pose of **16** (blue) with fucosidase of *B. taurus*.

2.4. Cell assays

2.4.1. Cytotoxicity against BT-474, MCF-7 and DU-145 cell lines using the MTT Assay

The BT-474 (breast cancer), MCF-7 (breast cancer) and DU-145 (prostate cancer) cell lines, available at the National University of Ireland Galway (NUI Galway), were used to independently determine whether compounds **5**, **16**, **18**, **20** and **22** were cytotoxic using the MTT assay. Compound **16** was found to be the most toxic against all cell lines exhibiting a greater potency towards prostate cancer cell line (DU-145). Toxicity of pleurotin, a positive control, is also given in Table 5 [63,64].

2.4.2. Inhibition of proliferation of human head and neck carcinoma cell lines

Compound **16** was further tested for its inhibition of proliferation of human head and neck carcinoma cells (HNO41, HNO97, HNO210), as well that of patient-derived glioblastoma-initiating cells (NCH644 IDH1-wt GBM) using the CellTiter-Glo assay. Compound **16** inhibited the proliferation of all these cell lines with IC_{50} values ranging from 12 µM to 17.6 µM (Table 6). The inhibition by puromycin, a positive control, is also reported for these various cell types.

3. Conclusions

A series of *N*-alkylated fuconojirimycin analogues have been prepared and evaluated as inhibitors of fucosidases of bacterial and bovine origin. The best inhibitory activity for the new compounds, was observed for *N*-decyl-DFJ against the bovine fucosidase (IC_{50} = 2.5 µM). The pairwise sequence alignment for the two enzymes showed their close resemblance, sharing evolutionary conserved domains. Homology models of the fucosidases from human and bovine origin were thus both constructed and used in docking and molecular dynamics. *N*-Decyl-DFJ was shown to inhibit growth of various cell lines, including IDH wild type glioblastoma cells [64] and could form the basis for development of more potent inhibitors of tumour cell growth.

4. Experimental section

4.1. General methods for preparative chemistry

Optical rotations were determined with a Perkin-Elmer 343 model polarimeter at the sodium D line at 20 °C. Deuterated chloroform ($CDCl_3$), CD_3OD or D_2O were used as NMR solvents, unless otherwise stated. NMR spectra were recorded (30 °C) with 400 or 500 MHz spectrometers. Chemical shifts are reported relative to internal Me_4Si in $CDCl_3$ (δ 0.0) or HOD for D_2O (δ 4.79) or CD_2HOD (δ 3.31) for ^1H and Me_4Si in $CDCl_3$ (δ 0.0) or $CDCl_3$ (δ 77.0) or CD_3OD (δ 49.05) for ^{13}C. ^1H NMR signals were assigned with the aid of COSY. ^{13}C NMR signals were assigned with the aid of DEPT, gHSQCAD and/or gHMBCAD. Coupling constants are reported in hertz. Splitting patterns are designated as follows: s, singlet; d, doublet; t, triplet; q, quartet; m, multiplet and br, broad. Low and high-resolution mass spectra were in positive and/or negative mode as indicated in each case. All anhydrous reactions were performed in flame-dried or oven-dried glassware under a positive pressure of dry argon or nitrogen. Air or moisture-sensitive reagents and anhydrous solvents were transferred with oven-dried syringes or

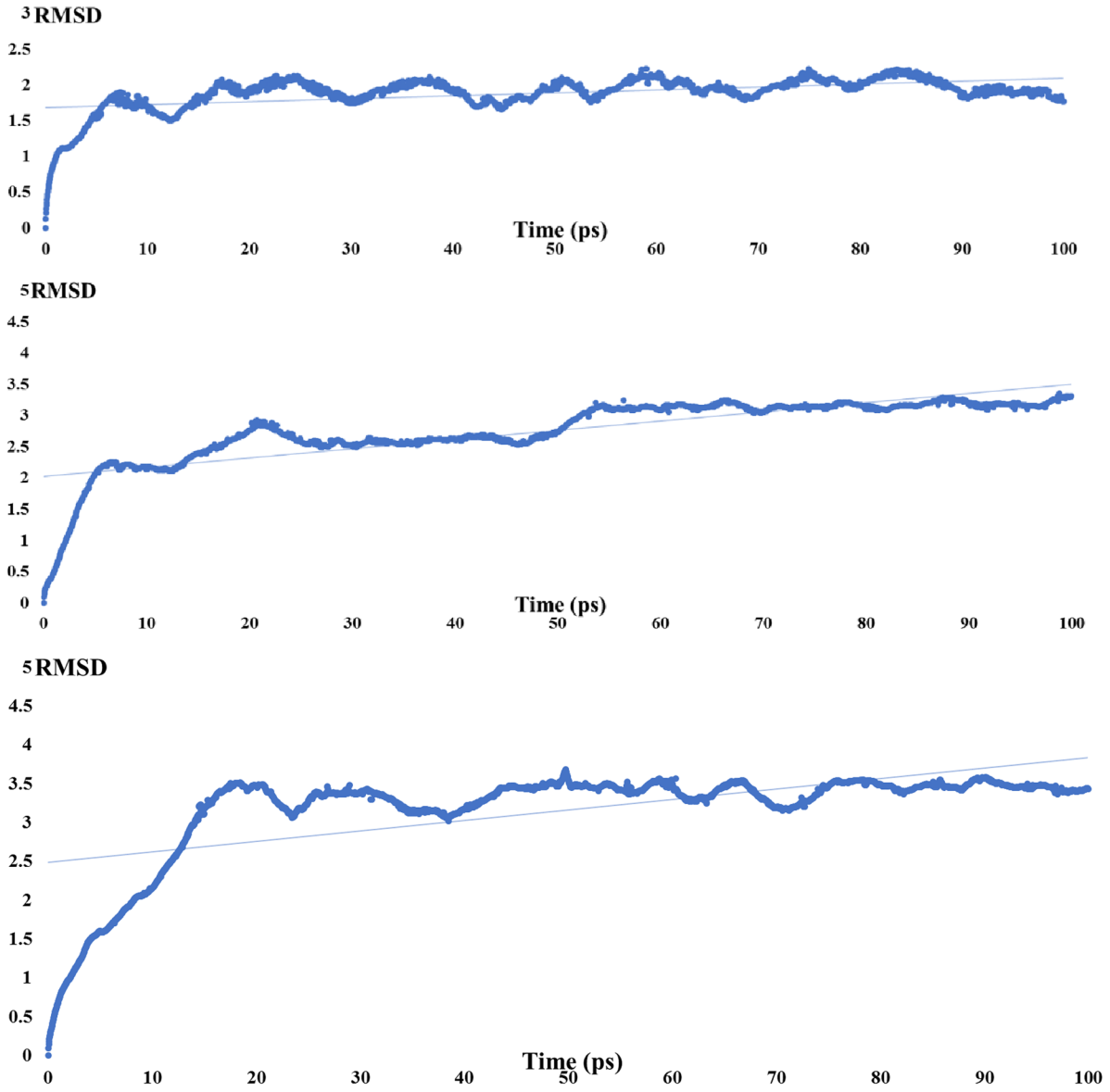

Fig. 6. MD run over 100 ps, (A) compound **2** (with fucosidase of *T. maritima*) with RMSD 1.88 Å; (A) Compound **2** with *B. taurus* fucosidase has RMSD 2.76 Å (C) Compound **16** with *B. taurus* fucosidase had an RMSD of 3.20 Å.

cannulae. All flash chromatography was performed with E. Merck silica gel 60 (230–400 mesh). All solution phase reactions were monitored using analytical thin layer chromatography (TLC) with 0.2 mm pre-coated silica gel aluminum plates 60 F254. Components were visualized by illumination with a short-wavelength (254 nm) ultraviolet light and/or staining (ceric ammonium molybdate, potassium permanganate, or phosphomolybdate stain solution). Flash chromatography was carried out with silica gel 60 (0.040–0.630 mm) and using a stepwise solvent polarity gradient correlated with TLC mobility. CH_2Cl_2, MeOH, toluene, CH_3CN and THF reaction solvents were used as obtained from a Pure Solv™ Solvent Purification System. Anhydrous DMF, pyridine were used as purchased. Chromatography solvents were used as obtained from suppliers. All other reagents were obtained from Sigma-Alrich unless otherwise stated.

4.2. Experimental procedures

4.2.1. N-Benzyl-2,3-di-O-benzyl-1,5,6-trideoxy-1,5-imino-D-altritol 9 And N-benzyl-2,3-di-O-benzyl-1,5-dideoxy-1,5-imino-L-fucitol 10

Compound **7** (39 mg, 0.11 mmol) was dissolved in MeOH (2 mL). Benzylamine (20 μL, 0.17 mmol) in MeOH (1 mL) was mixed with acetic acid (13 μL, 0.22 mmol) to adjust the pH value to 4–5, and this solution was added to the reaction mixture over a period of 0.5 h by cooling over an ice-water bath. A portion of $NaBH_3CN$ (22 mg, 0.33 mmol) was then added, and the mixture was stirred for 18 h at room temp. The mixture was quenched with 0.5 mL 1 N HCl aqueous solution. After removal of the solvent, the residue was dissolved in 10% Na_2CO_3 (10 mL), and extracted with EtOAc (3 × 7 mL). The EtOAc layers were combined, dried (Na_2SO_4), filtered, and the solvent was removed. Chromatography of the residue on silica gel gave **9** (16 mg, 36%) and compound **10** (19 mg, 40%); **9** was eluted with cyclohexane-EtOAc (7:1), while **10** was eluted with cyclohexane-EtOAc (5:1).

Analytical data for 9: $[\alpha]_D^{20}$ −14.6 (*c* 1.6, $CHCl_3$); ^{1}H NMR (500 MHz, $CDCl_3$) δ 7.25–7.33(m, 15H, H_{Ar}), 4.69 (d, J = 11.7 Hz, 1H, PhC*H*H), 4.64 (d, J = 11.7 Hz, 1H, PhC*H*H), 4.57 (d, J = 11.7 Hz, 1H, PhC*H*H), 4.53 (d, J = 11.7 Hz, 1H, PhC*H*H), 3.78 (d, J = 13.0 Hz, 1H, PhC*H*H), 3.76 (m, 1H, H_2), 3.72 (dd, J = 4.6, 3.4 Hz, 1H, H_4), 3.62 (dd, J = 7.4, 3.4 Hz, 1H, H_3), 3.50 (d, J = 13.0 Hz, 1H, PhC*H*H), 2.91 (m, 1H, H_5), 2.67 (dd, J = 12.0, 4.5 Hz, 1H, $H_{1\text{-eq}}$), 2.55 (dd, J = 12.0, 8.1 Hz, 1H, $H_{1\text{-ax}}$), 1.69 (s, 1H, OH), 1.09 (d, J = 6.70 Hz, 1H, CH_3), ^{13}C

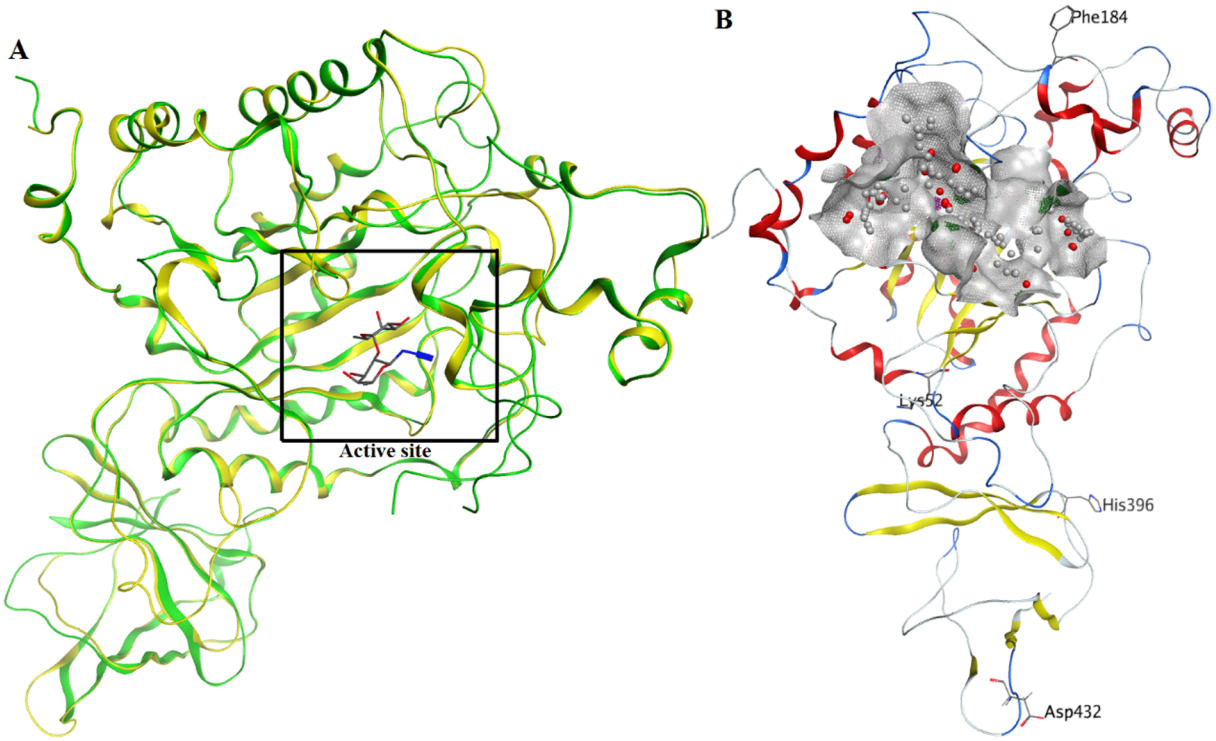

Fig. 7. (A) The RMSD value between the template (2WSP, yellow) and the human fucosidase homology model (green), which are superposed, was 0.71. The black rectangle outlines the active site. (B) The binding site is shown in grey. The red spheres are atoms with potential to interact with hydrophobic groups, whereas the grey spheres correspond to atoms that have potential as H-bonding donors/acceptors.

NMR (125 MHz, $CDCl_3$) δ 138.82, 138.55, 138.36 (each C), 128.68, 128.38, 128.34, 128.31, 128.15, 127.78, 127.69, 127.67, 127.53, 127.08, 126.95 (each CH), 78.84 (C_3), 74.95 (C_2), 72.27 (Ph*C*H_2), 71.36 (C_4), 57.83 (Ph*C*H_2), 57.80 (C_5), 48.77 (C_1), 10.42 (CH_3, C_6); HRMS: Calcd for $C_{27}H_{32}NO_3$, $[M + H]^+$, 418.2387; Found, 418.2386.

Analytical data for 10: $[\alpha]_D^{20}$ 16.4 (*c* 1.0, $CHCl_3$); ^{1}H NMR (500 MHz, $CDCl_3$) δ 7.41–7.20 (m, 15H, H_{Ar}), 4.74 (dd, J = 14.0, 12.0 Hz, 2H, PhC*H*$_2$), 4.67 (d, J = 11.6 Hz, 1H, PhC*H*H), 4.53 (d, J = 11.6 Hz, 1H, PhC*H*H), 3.95 (d, J = 13.6 Hz, 1H, PhC*H*H), 3.82 (dd, J = 3.1, 1.4 Hz, 1H, H_4), 3.81–3.75 (m, 1H, H_2), 3.32 (dd, J = 9.1, 3.2 Hz, 1H, H_3), 3.29 (d, J = 13.6 Hz, 1H, PhC*H*H), 2.99 (dd, J = 11.5, 5.1 Hz, 1H, $H_{1\text{-eq}}$), 2.48–2.37 (m, 1H, H_5), 1.94–1.84 (m, 1H, $H_{1\text{-ax}}$), 1.34 (d, J = 6.5 Hz, 3H, CH_3). ^{13}C NMR (125 MHz, $CDCl_3$) δ 138.81, 138.64, 138.34 (each C), 129.06, 128.51, 128.46, 128.41, 127.90, 127.78, 127.76, 127.63, 127.22 (each CH), 83.45 (C_3), 75.88 (C_2), 73.13 (Ph*C*H_2), 72.18 (Ph*C*H_2), 72.05 (C_4), 58.88 (C_5), 56.81 (Ph*C*H_2), 54.84 (C_1), 16.94 (CH_3, C_6). HRMS: Calcd for $C_{27}H_{32}NO_3$, $[M + H]^+$, 418.2387; Found, 418.2382.

4.2.2. N-((R)-1-Phenylethyl)-2,3-di-O-benzyl- 1,5,6-trideoxy-1,5-imino-D-altritol (11)

Compound **7** (29 mg, 0.085 mmol) was dissolved in methanol. (*R*)-Phenylethanamine (22 µL, 0.17 mmol) in MeOH (1 mL) was treated with acetic acid to adjust the pH value to 4–5, and this solution was added to the reaction mixture at room temp. A portion of $NaBH_3CN$ (16 mg, 0.25 mmol) was then added, and the mixture was stirred at 60 °C for 2 hr then left at room temp overnight. The mixture was quenched with 0.5 mL 1 N HCl aqueous solution. After removal of the solvent, the residue was dissolved in 10% Na_2CO_3 (8 mL), and extracted with EtOAc (3 × 6 mL). The EtOAc layers were combined, dried (Na_2SO_4), filtered, and the solvent was removed. Chromatography of the residue on silica gel (cyclohexane-EtOAc, 8:1) gave **11** (31 mg,

Table 4
Comparison of scores attained from docking placement methods against the IC_{50}/K_D values for the compounds against human fucosidase (HuF) and *T. maritima* fucosidase™.

Compd	K_i/IC_{50} for HuF (µM)	K_i/IC_{50} for TM (µM)	Alpha Triangle Method		Triangle Matcher Method		Alpha PMI Method	
			HuF[a]	TM[b]	HuF[a]	TM[b]	HuF[a]	TM[b]
23	0.0056[c]	0.000105[c]	−12.037	−12.114	−11.887	−12.199	−13.011	−12.357
24	0.0097[c]	0.000259[c]	−11.451	−11.78	−11.764	−12.002	−12.882	−12.41
25	0.0117[c]	0.00119[c]	−11.393	−11.491	−11.119	−11.833	−12.50	−12.042
26	0.018[c]	0.00101[c]	−11.108	−11.542	−10.810	−11.809	−12.619	−11.945
27	0.018[d]	0.052[d]	−10.920	−11.304	−10.991	−10.892	−12.451	−11.807
28	0.035[d]	0.064[d]	−10.543	−10.928	−10.605	−10.712	−11.521	−11.065
29	0.092[d]	0.070[d]	−10.008	−10.637	−9.332	−10.288	−11.402	−10.42
30	0.106[d]	0.267[d]	−10.219	−10.419	−9.290	−9.074	−11.477	−10.317

[a] Human fucosidase homology model.
[b] fucosidase of *T. maritima.*
[c] *Ki* values in µM.
[d] IC_{50} values in µM.

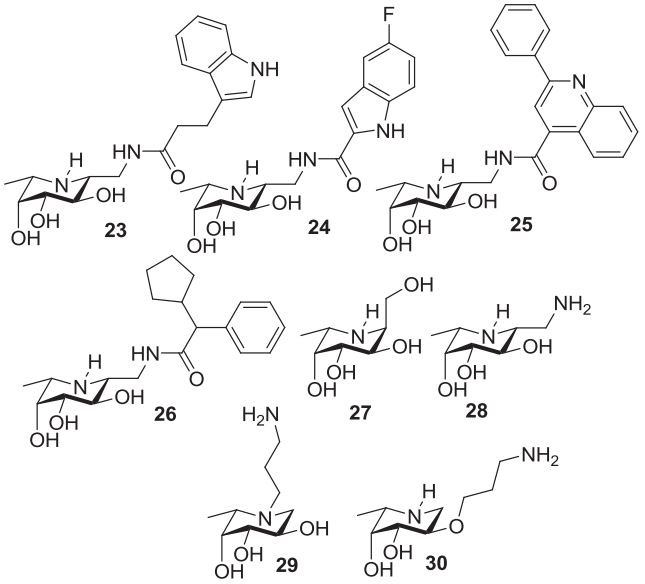

Fig. 8. The compounds of Ho et al. [34] used in the docking study.

85%) as a white solid; $[\alpha]_D^{20}$ −1.8 (*c* 1.0, $CHCl_3$); ^{1}H NMR (500 MHz, $CDCl_3$) δ 7.39–7.13 (m, 15H, H_{Ar}), 4.70 (d, *J* = 11.9 Hz, 2H, PhCH_2,), 4.45 (d, *J* = 11.7 Hz, 1H, PhC*H*H), 4.36 (d, *J* = 11.7 Hz, 1H, PhC*H*H), 3.82–3.72 (m, 2H, 1x NPhC*H*H & H_4), 3.65 (td, *J* = 8.3, 4.7 Hz, 1H, H_2), 3.60 (dd, *J* = 7.9, 3.1 Hz, 1H, H_3), 3.38–3.29 (m, 1H, H_5), 2.75 (d, *J* = 6.6 Hz, 1H, OH), 2.63 (dd, *J* = 12.1, 4.5 Hz, 1H, $H_{1\text{-eq}}$), 2.29 (dd, *J* = 12.1, 8.6 Hz, 1H, $H_{1\text{-ax}}$), 1.28 (d, *J* = 6.7 Hz, 3H, CH_3), 1.05 (d, *J* = 6.8 Hz, 3H, CH_3); ^{13}C NMR (125 MHz, $CDCl_3$): δ 145.61 (C), 138.68 (C), 138.64 (C), 128.54 (CH), 128.52 (CH), 128.38 (CH), 127.96 (CH), 127.79 (CH), 127.73 (CH), 127.58 (CH), 127.26 (CH), 127.06 (CH), 79.43 (C_3), 75.59 (C_2), 72.41 ($PhCH_2$), 72.34 ($PhCH_2$), 71.57 (C_4), 59.12 (PhC*H*(CH_3)N), 54.89 (C_5), 45.84 (C_1), 19.19 (PhCH(C*H*$_3$)N), 9.78 (CH_3, C_6). IR (film, $CHCl_3$): ν_{max} 3025, 2920, 2358, 1450, 1369, 1260, 1205, 1092, 799, 738, 698; ES-HRMS: Found 432.2523, $C_{28}H_{34}NO_3$ requires 432.2539 $[M + H]^+$.

4.2.3. *N-Benzyl-2,3,4-tri-O-benzyl -1,5 -dideoxy-1,5-imino-L-fucitol (14a)*

The diol **13** (95 mg, 0.46 mmol) was dissolved in CH_2Cl_2 (8 mL), and triethylamine (0.14 mL, 1.01 mmol) was added and the solution was cooled to 0 °C, methanesulfonyl chloride (75 μL, 0.96 mmol) was added dropwise and stirred for 4 h. The solvent was removed under reduced pressure and the residue was used for next step without further purification. The bis-mesylate was dissolved in THF (1 mL) and benzylamine (0.2 mL, 1.84 mmol) was added at room temp, and the mixture was heated at 40 °C for 8 h, after which TLC indicated complete consumption of the bis-mesylate. The solution was cooled to room temp, and the solvent removed under reduced pressure. The residue was dissolved in EtOAc (30 mL), and washed with 2 M NaOH (2 × 20 mL). The organic phase was separated, further washed with brine and dried with Na_2SO_4. Removal of the solvent under reduced pressure and flash column chromatography of the residue on silica gel (cyclohexane-EtOAc, 10:1) gave **14a** (80 mg, 77%) as a colourless oil; R_f 0.65 (cyclohexane-EtOAc, 4:3); $[\alpha]_D^{20}$ −9.4 (*c* 0.85, $CHCl_3$); ^{1}H NMR (500 MHz, $CDCl_3$) δ 7.45–7.17 (m, 20H, H_{Ar}), 4.91 (d, *J* = 11.8 Hz, 1H, PhC*H*H), 4.82–4.71 (m, 2H, PhCH_2), 4.66 (d, *J* = 11.8 Hz, 1H, PhC*H*H), 4.62 (d, *J* = 11.7 Hz, 1H, PhC*H*H), 4.55 (d, *J* = 11.7 Hz, 1H, PhC*H*H), 3.93 (d, *J* = 3.6 Hz, 1H, H_2), 3.85–3.69 (m, 2H, PhC*H*H & H_4), 3.59 (d, *J* = 14.0 Hz, 1H, PhC*H*H), 3.47 (d, *J* = 6.5 Hz, 1H, H_3), 3.00 (dd, *J* = 11.9, 4.0 Hz, 1H, $H_{1\text{-eq}}$), 2.62 (m, 1H, H_5), 2.22–2.06 (m, 1H, $H_{1\text{-ax}}$), 1.21 (d, *J* = 6.5 Hz, 3H, CH_3); ^{13}C NMR (125 MHz, $CDCl_3$): δ 139.21, 138.99, 138.23 (each C), 129.38, 128.43, 128.40, 128.31, 128.28, 128.26, 127.75, 127.55, 127.54, 127.51, 127.03 (each CH), 83.37 (C_3), 79.10 (C_4), 75.83 (C_2), 74.29 ($PhCH_2$), 73.11 ($PhCH_2$), 72.51 ($PhCH_2$), 57.36 (C_5), 57.04 ($PhCH_2$), 52.58 (C_1), 14.98 (CH_3, C_6); ES-HRMS: Found 508.2844, $C_{34}H_{38}NO_3$ $[M + H]^+$ requires 508.2852.

4.2.4. *N-Decyl-2,3,4-tri-O-benzyl- 1,5 -dideoxy-1,5-imino-L-fucitol (14b)*

Reaction of the bis-mesylate (58 mg, 0.098 mmol) as described in the preparation of **14a** with *n*-decylamine gave **14b** (45 mg, 83%) as a white solid after column chromatography (cyclohexane-EtOAc, 7:1); $[\alpha]_D^{20}$ 12.0 (*c* 1.0, $CHCl_3$); ^{1}H NMR (500 MHz, $CDCl_3$) δ 7.43–7.21 (m, 15H, H_{Ar}), 4.91 (d, *J* = 12.0, 1H, 1 × PhC*H*H), 4.73 (m, 5H, 5 × PhC*H*H), 4.04–3.92 (m, 1H, H_2), 3.64 (m, 1H, H_4), 3.41 (d, *J* = 7.0, 1H, H_3), 3.08 (dd, J = 10.0, 4.5, 1H, $H_{1\text{-eq}}$), 2.63–2.45 (m, 2H, CH_2), 2.41 (m, 1H, H_5), 2.23 (t, *J* = 10.0, 1H, $H_{1\text{-ax}}$), 1.47–1.08 (m, 16H, 8 × CH_2), 1.00 (d, *J* = 6.5, 3H, NCHCH_3), 0.88 (t, *J* = 6.5, 3H, CH_2CH_3). ^{13}C NMR (125 MHz, $CDCl_3$) δ 139.06 (C), 138.91 (C), 128.74, 128.30, 128.28, 128.05, 127.74, 127.46, 127.44, 127.38 (each CH), 84.31(C_3), 78.54 (C_4), 76.32(C_2), 74.38 ($PhCH_2$), 73.03 ($PhCH_2$), 72.75 ($PhCH_2$), 57.12 (C_5), 54.15 (NCH_2Ph), 53.19 (C_1), 31.89, 30.32, 29.62, 29.59, 29.55, 29.31, 27.66, 22.66 (each CH_2), 15.49 (CH_3, C_6), 14.09

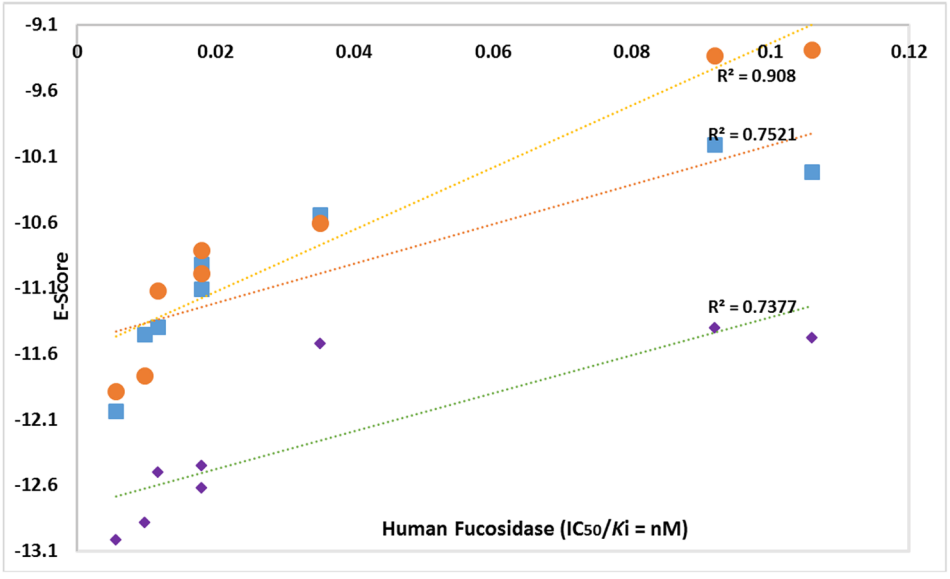

Fig. 9. Plots of docking E-score (y-axis) and K_i/IC_{50} values (nM) for human fucosidase (x-axis) for three docking placement methods (see Table 4 for data used).

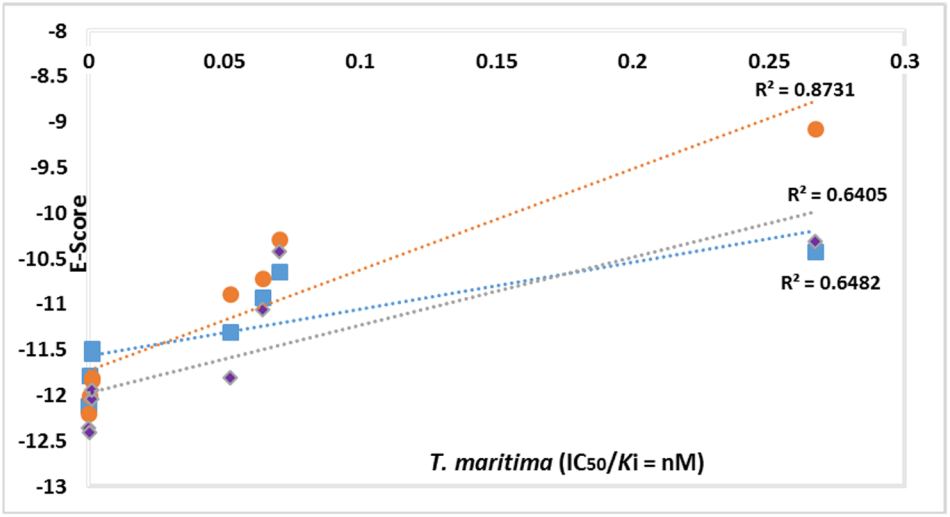

Fig. 10. Plots of E-score (y-axis) and K_i/IC_{50} values (x-axis) for inhibitors of the *T. maritima* fucosidase for three docking placement methods (see Table 4 for data used).

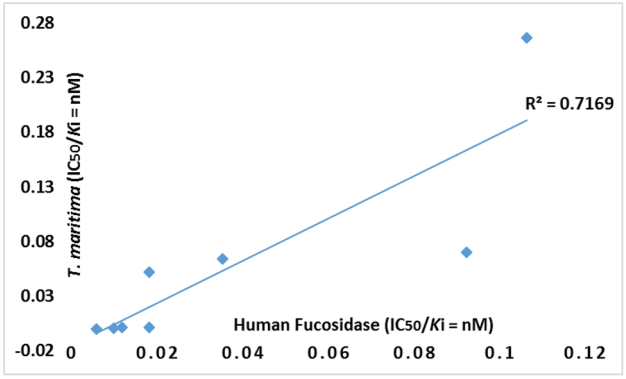

Fig. 11. Plots of IC_{50}/K_D values for inhibitors of human fucosidase (x-axis) versus those of *T. maritima* fucosidase (y-axis, see Table 4 for the data used).

(CH_3). IR (film, $CHCl_3$): ν_{max} 3661, 2924, 2346, 1732, 1455, 1365, 1096, 734 cm^{-1}; HRMS: Calcd for $C_{37}H_{52}NO_3$, $[M + H]^+$, 558.3947; Found, 558.3975.

4.2.5. N-Octyl-2,3,4-tri-O-benzyl-1,5 -dideoxy-1,5-imino-L-fucitol (14c)

Reaction of the bis-mesylate (44 mg, 0.074 mmol) as described in the preparation of **14a** with *n*-octylamine gave **14c** (33 mg, 80%) as a white solid after chromatography (cyclohexane-EtOAc, 8:1); $[\alpha]_D^{20}$ 11.2 (*c* 1.5, $CHCl_3$); ^1H NMR (500 MHz, $CDCl_3$) δ 7.42–7.21 (m, 15H, H_{Ar}), 4.91 (d, J = 12.0, 1H, 1 × PhC*H*H), 4.83–4.62 (m, 5H, 5 × PhC*H*H), 3.99 (td, J = 9.0, 4.5, 1H, H_2), 3.64 (s, 1H, H_4), 3.41 (dd, J = 9.0, 2.5, 1H, H_3), 3.08 (dd, J = 11.5, 4.5, 1H, $H_{1\text{-eq}}$), 2.53 (m, 2H, CH_2), 2.41 (m, 1H, H_5), 2.23 (t, J = 10.5, 1H, $H_{1\text{-ax}}$), 1.48–1.35 (m, 1H, 1 × C*H*HCH$_2$), 1.35–1.07 (m, 11*H*, 11 × C*H*HCH$_2$), 1.00 (d, J = 6.5, 3H, CHCH_3), 0.87 (t, J = 7.0, 3H, CH$_2$CH_3); ^{13}C NMR (125 MHz, $CDCl_3$) δ 139.07, 138.92 (each C), 128.74, 128.31, 128.29, 128.06, 127.75, 127.47, 127.46, 127.45, 127.39 (each CH), 84.26 (C_3), 78.56 (C_4), 76.32 (C_2), 74.39 (PhCH$_2$), 73.03 (PhCH$_2$), 72.75 (PhCH$_2$), 57.13 (C_5), 54.14 (C_1), 53.19 (NCH$_2$Ph), 31.82, 29.56, 29.28, 27.67, 23.19, 22.65 (each CH$_2$), 15.70 (CH_3-C_6), 14.09 (CH_3); IR (film, $CHCl_3$): νmax 3389, 3034, 2925, 2347, 1955, 1603, 1455, 1367, 1269, 1096 cm^{-1}. HRMS: Calcd for $C_{35}H_{48}NO_3$, $[M + H]^+$, 530.3634; Found, 530.3654.

4.2.6. N-Butyl -2,3,4-tri-O-benzyl- 1,5 -dideoxy-1,5-imino-L-fucitol (14d)

Compound **14d** was prepared from bis-mesylate (81 mg, 0.136 mmol) as described in the preparation of **14a**, yielding **14d** (50 mg, 78%) as white solids after column chromatography (cyclohexane-EtOAc 8:1); $[\alpha]_D^{20}$ 16.4 (*c* 1.0, $CHCl_3$); ^1H NMR (500 MHz, $CDCl_3$) δ 7.42–7.22 (m, 15H, H_{Ar}), 4.92 (d, J = 11.8 Hz, 1H, 1 × PhC*H*H), 4.80 (d, J = 12.0 Hz, 1H, 1 × PhC*H*H), 4.71 (m, 4H, 4 × PhC*H*H), 3.99 (td, J = 9.0, 4.5 Hz, 1H, H_2), 3.65 (t, J = 2.3 Hz, 1H, H_4), 3.41 (dd, J = 8.8, 2.7 Hz, 1H, H_3), 3.08 (dd, J = 11.0, 4.5 Hz, 1H, $H_{1\text{-eq}}$), 2.58 (ddd, J = 13.6, 11.0, 5.0 Hz, 1H, NC*H*HCH$_2$), 2.50 (ddd,

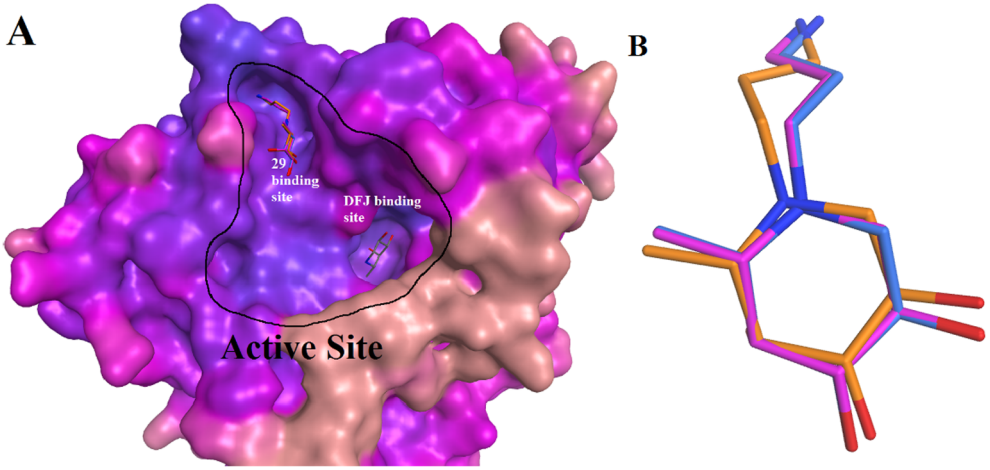

Fig. 12. (A) The black contour line outlines the active binding site in fucosidase of *T. maritima*. Here **29** was predicted to differ in binding position with respect to DFJ **2**; (B) The docked conformations of **29**, corresponding to the three docking methods, are shown overlayed in blue (triangle matcher), magenta (alpha triangle), orange (alpha PMI).

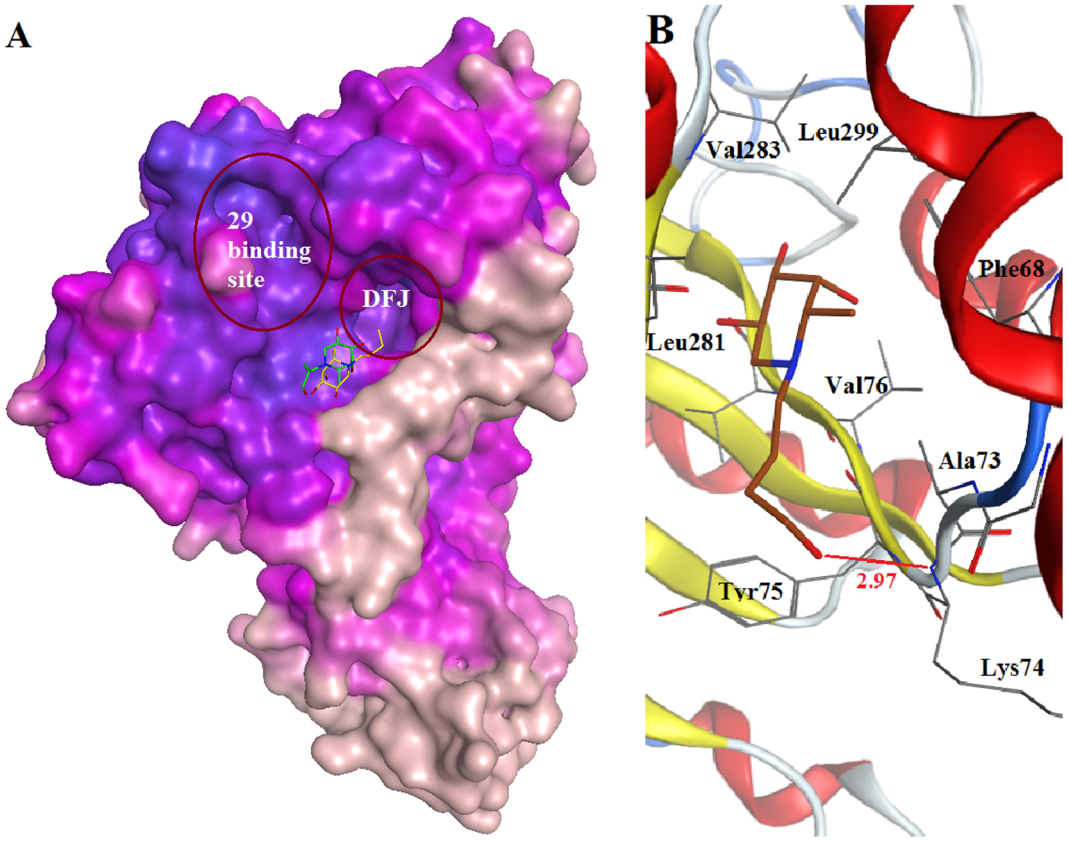

Fig. 13. (A) The binding of **18** (yellow colour) and **22** (cyan colour) in fucosidase of *T. maritima*. This showed **18** and **22** outside the binding regions predicted to be occupied by **29** and **DFJ**. (B) The docking pose of **22** with respect to the fucosidase of *B. taurus* shown with predicted H-bonding interaction (green line) of Lys74.

J = 13.6, 11.0, 5.0 Hz, 1H, NCH*H*CH_2), 2.41 (m, 1H, H_5), 2.23 (dd, J = 11.0, 9.8 Hz, 1H, $H_{1\text{-}ax}$), 1.48–1.16 (m, 4H, 2 × CH_2), 1.01 (d, J = 6.5 Hz, 3H, CHCH_3), 0.89 (t, J = 7.3 Hz, 3H, CH_2CH_3); ^{13}C NMR (125 MHz, $CDCl_3$) δ 139.05 (C), 138.90 (C), 128.73, 128.29, 128.28, 128.05, 127.74, 127.46, 127.43, 127.38 (each CH), 84.48 (C_3), 78.56 (C_4), 76.31 (C_2), 74.39 (PhCH_2), 73.02 (PhCH_2), 72.74 (PhCH_2), 57.13 (C_5), 54.27(C_1), 52.86 (NCH_2), 25.33 (CH_2), 20.81(CH_2), 15.36 (CH_3-C_6), 14.04 (CH_2CH_3); HRMS: Calcd for $C_{31}H_{40}NO_3$, $[M + H]^+$, 474.3008; Found, 474.3024.

4.2.7. *N-(2-(Benzyloxy)ethyl)-2,3,4-tri-O-benzyl-1,5-dideoxy-1,5-imino-L-fucitol (14e)*

Compound **14e** was prepared from bis-mesylate (85 mg, 0.144 mmol) as described in the preparation of **14a**, yielding **14e** (60 mg, 75%) as white solids after column chromatography (cyclohexane-EtOAc4:1); $[\alpha]_D^{20}$ 2.9 (*c* 1.25, $CHCl_3$); ^{1}H NMR (500 MHz, $CDCl_3$) δ 7.41–7.22 (m, 20H, H_{Ar}), 4.91 (d, J = 12.0, 1H, 1 × PhC*H*H), 4.80 (d, J = 12.0, 1H, 1 × PhC*H*H), 4.77–4.66 (m, 3H, 3 × PhC*H*H), 4.64 (d, J = 12.0, 1H, 1 × PhC*H*H), 4.47 (s, 2H, 2 × PhC*H*H), 3.97 (td, J = 9.0, 4.5, 1H, H_2), 3.65 (m, 1H, H_4), 3.61–3.48 (m, 2H, NC$H_2$$CH_2$), 3.43 (dd, J = 9.0, 2.5, 1H, H_3), 3.16 (dd, J = 11.0, 4.5, 1H, $H_{1\text{-}eq}$), 2.93–2.78 (m, 2H, CH_2OBn), 2.54 (m, 1H, H_5), 2.42 (t, J = 11.0, 1H, $H_{1\text{-}ax}$), 1.05 (d, J = 6.5, 3H, CH_3). ^{13}C NMR (125 MHz, $CDCl_3$) δ 139.04 (C), 138.86 (C), 138.38 (C), 128.65, 128.33, 128.30, 128.27, 128.07, 127.73, 127.54, 127.50, 127.45, 127.38 (each CH), 84.48 (C_3), 78.56 (C_4), 76.00 (C_2), 74.39 (PhCH_2), 73.18 (PhCH_2), 73.04 (PhCH_2), 72.67 (PhCH_2), 67.21(NCH_2), 57.72 (C_5), 54.38 (C_1), 51.94 (CH_2), 15.74 (CH_3, C_6). ES-HRMS: Found 552.3114, $C_{36}H_{42}NO_4$ $[M + H]^+$ requires 552.3122.

4.2.8. *N-(2-Aminoethyl)-2,3,4-tri-O-benzyl-1,5-dideoxy-1,5-imino-L-fucitol (14f)*

Compound **14f** was prepared from bis-mesylate (130 mg, 0.22 mmol) as described in the preparation of **14a**, yielding **14f** (82 mg, 81%) as white foam after column chromatography (cyclohexane/EA 2:1); $[\alpha]_D^{20}$ −0.8 (*c* 2.3, $CHCl_3$); ^{1}H NMR (600 MHz, $CDCl_3$) δ 7.38–7.25 (m, 15H, H_{Ar}), 4.89 (d, J = 11.4, 1H, 1 × PhC*H*H), 4.62–4.81 (m, 5H, 5 × PhC*H*H), 3.96 (m, 1H, H_2), 3.70 (m, 1H, H_4), 3.48 (dd, J = 7.2, 1.5, 1H, H_3), 3.08 (dd, J = 10.5, 3.5, 1H, $H_{1\text{-}eq}$), 2.80–2.66 (m, 3H, NC*H*HCH_2 & CH_2NH_2), 2.55 (m, 1H, H_5), 2.42 (t, J = 6.0, 1H, NC*H*HCH_2), 2.21 (t, J = 10.5, 1H, $H_{1\text{-}ax}$), 1.09 (d, J = 6.5, 3H, CH_3). ^{13}C NMR (150 MHz, $CDCl_3$) δ 139.03 (C), 138.92 (C), 138.81(C), 128.34, 128.32, 128.26, 128.18, 127.73, 127.53, 127.50, 127.46, 127.42 (each CH), 83.16 (C_3), 78.87 (C_4), 75.86 (C_2), 74.20 (PhCH_2), 73.04 (PhCH_2), 72.67 (PhCH_2), 57.96 (C_5), 55.51(CH_2), 53.12 (C_1), 38.13 (CH_2), 14.66 (CH_3). IR (film, $CHCl_3$): νmax 3360, 2915, 1364, 1095 cm^{-1}. ES-HRMS: Found 461.2802, $C_{29}H_{37}N_2O_3$ $[M + H]^+$ requires 461.2804.

4.2.9. *N-Allyl- 2,3,4-tri-O-benzyl-1,5-dideoxy-1,5-imino-L-fucitol (14g)*

Compound **14g** was prepared from bis-mesylate (90 mg, 0.15 mmol) as described in the preparation of **14a**, yielding **14g** (59 mg, 85%) as colorless oil after column chromatography (cyclohexane/EA 6:1); R_f 0.52 (cyclohexane-EtOAc, 2:1); ^{1}H NMR (500 MHz, $CDCl_3$) δ 7.56–7.09 (m, 15H, H_{Ar}), 5.97–5.77 (m, 1H, $NCH_2CH = CH_2$), 5.19–5.08 (m, 2H, $NCH_2CH = CH_2$), 4.92 (d, J = 11.8 Hz, 1H, 1 × PhC*H*H), 4.85–4.61 (m, 5H, 5 × PhC*H*H), 4.10–3.94 (m, 1H, H_2), 3.66 (s, 1H, H_4), 3.42 (dd, J = 7.6, 1.0 Hz, 1H, H_3), 3.26 (dd, J = 14.3, 6.0 Hz, 1H, NC*H*HCH = CH_2), 3.16–3.02 (m, 2H, $H_{1\text{-}eq}$ & NC*H*HCH = CH_2), 2.41 (m, 1H, H_5), 2.19 (t, J = 10.4 Hz, 1H, $H_{1\text{-}ax}$), 1.03 (d, J = 6.4 Hz, 3H, CH_3). ^{13}C NMR (125 MHz, $CDCl_3$) δ 139.17,

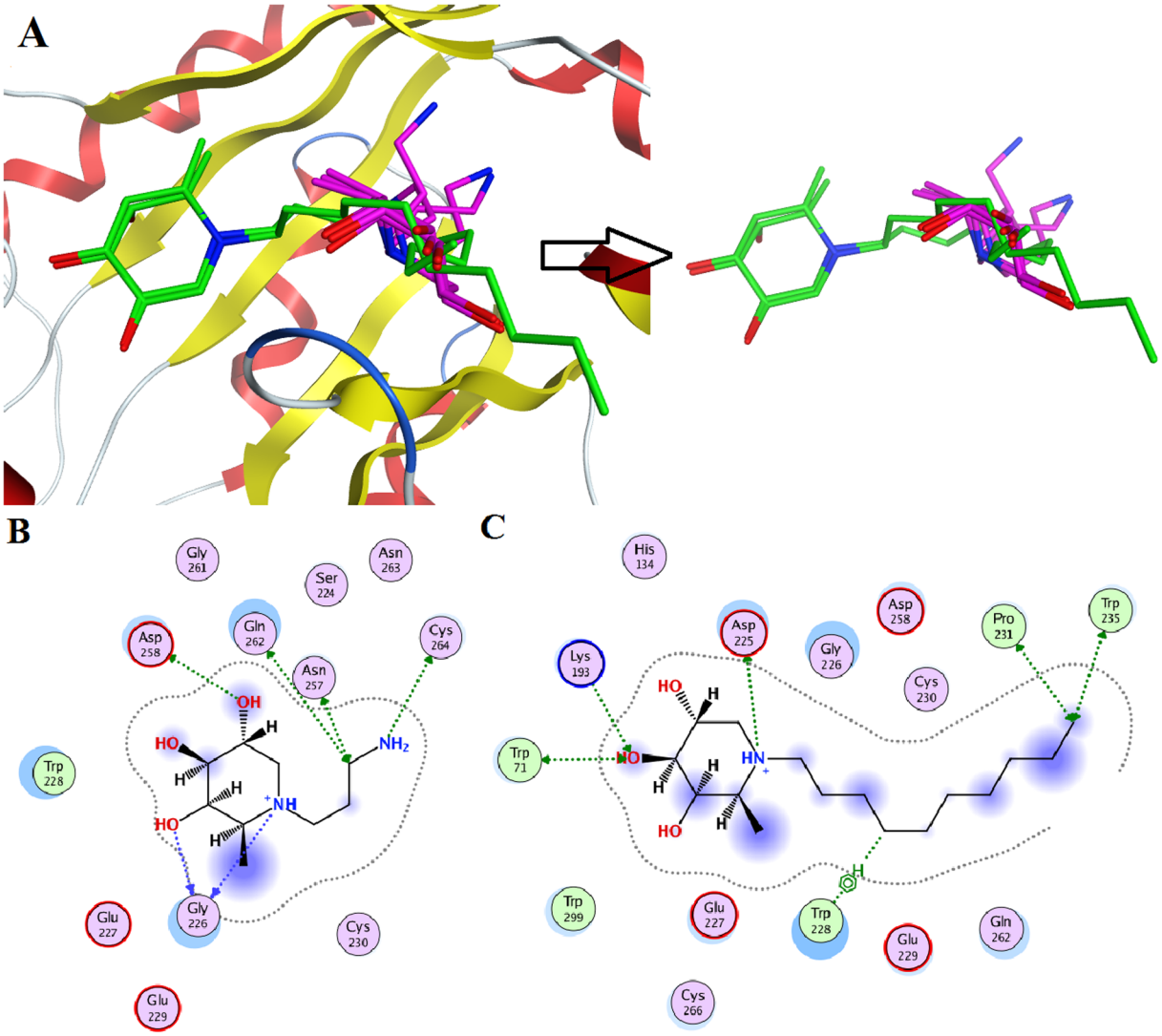

Fig. 14. (A) The predicted binding of **29** (purple) and **16** (green) in the fucosidase of human origin, along with the clustered conformations. The predicted 2-D interaction of **29** (**B**) and **16** (**C**) with human fucosidase.

Table 5
Cytotoxicity evaluation using the MTT colorimetric assay. IC_{50} values were obtained after the incubation of cells with the test compounds in DMSO for 72 h.

Compound	IC_{50} BT-474 (μM)	IC_{50} MCF-7 (μM)	IC_{50} DU-145 (μM)
Pleurotin (control)	1.94 ± 0.49*	0.28 ± 0.03*	0.43 ± 0.06*
5	> 100	> 100	> 100
16	57.39 ± 3.38	30 ± 0.04	13.54 ± 0.75
18	> 100	77 ± 1.53	60.99 ± 3.15
20	> 100	> 100	> 100
22	> 100	> 100	> 100

Table 6
Inhibition of proliferation of cancer cell lines by **16**.

Cell line	IC_{50} of 16 [μM]	IC_{50} of puromycin [μM]
NCH644	17.6	0.27
HNO210	17.4	0.16
HNO97	12.0	0.24
HNO41	13.8	0.24

139.00, 138.98 (each C), 133.64 ($CH_2CH = CH_2$), 128.92, 128.46, 128.43, 128.23, 127.89, 127.65, 127.62, 127.60, 127.56 (each CH), 118.38 ($CH_2CH = CH_2$), 84.24 (C_3), 78.64 (C_4), 76.26 (C_2), 74.56 ($PhCH_2$), 73.24($PhCH_2$), 72.87($PhCH_2$), 57.50 (C_5), 56.47(NCH_2CH), 54.39 (C_1), 15.44 (CH_3, C_6). ES-HRMS: Found 458.2702, $C_{30}H_{36}NO_3$ $[M + H]^+$ requires 458.2695.

4.2.10. N-((Adamantylcarbonylamino)-ethyl)-2,3,4-tri-O-benzyl-1,5-dideoxy-1,5-imino-L-fucitol (15)

The 1-adamantanecarboxylic acid (5.6 mg, 0.031 mmol) was dissolved in dry CH_2Cl_2, cooled to 0 °C and EDC (9.2 mg, 0.048 mmol), HOBt (6.3 mg, 0.048 mmol), and DMAP (5.7 mg, 0.048 mmol) were added. After stirring for 1hr, the amine **14f** (11 mg, 0.024 mmol) was added. The reaction was warmed to room temp and stirred for 24 h. The mixture was then quenched with NH_4Cl (sat.) and extracted with CH_2Cl_2. The organic fractions were washed with satd. $NaHCO_3$, brine and dried with Na_2SO_4. The crude product was purified by flash chromatography on silica gel eluting with cyclohexane-EtOAc(1:1) to yield **15** (13 mg, 88%); R_f 0.18 (cyclohexane-EA, 1:1); $[\alpha]_D^{20}$ −4.4 (*c* 1.5, $CHCl_3$); ^1H NMR (500 MHz, $CDCl_3$) δ 7.41–7.21 (m, 15H, H_{Ar}), 4.85 (d, J = 11.5 Hz, 1H, 1 × PhC*H*H), 6.32 (s, 1H, NH), 4.80–4.71 (m, 2H, 2 × PhC*H*H), 4.65 (m, 3H, 3 × PhC*H*H), 3.86 (s, 1H, H_2), 3.72 (s, 1H,

H_4), 3.54 (d, J = 5.7 Hz, 1H, H_3), 3.26 (d, J = 4.9 Hz, 2H, NCH_2CH_2), 3.06 (dd, J = 11.8, 3.4 Hz, 1H, $H_{1\text{-eq}}$), 2.71 (m, 2H, 1 × NC*H*HCH$_2$ & H_5), 2.52–2.39 (m, 1H, NC*H*HCH$_2$), 2.24 (m, 1H, $H_{1\text{-ax}}$), 1.93 (s, 3H, 3 × CH), 1.77 (d, J = 2.0 Hz, 6H, 3 × CH_2), 1.67 (d, J = 12.0 Hz, 3H, 3 × C*H*H), 1.60 (d, J = 12.0 Hz, 3H, 3 × C*H*H), 1.12 (d, J = 6.5 Hz, 3H, CH_3). ^{13}C NMR (125 MHz, $CDCl_3$) δ 178.12 (C═O), 139.13, 139.11, 138.81 (each C), 128.50, 128.46, 128.32, 127.98, 127.72, 127.58 (each CH), 84.18 (C_3), 78.69 (C_4), 75.88 (C_2), 73.94 ($PhCH_2$), 73.22 ($PhCH_2$), 72.59 ($PhCH_2$), 57.70 (C_5), 51.05 (NCH_2CH_2), 40.70 (C), 39.48, 39.38, 36.70, 36.62, 35.97, 28.29 (each CH_2), 28.25 (CH), 15.40 (CH_3). HRMS: Calcd for $C_{40}H_{50}N_2O_4$, $[M + H]^+$, 623.3849; Found, 623.3839.

4.2.11. 1,5-Dideoxy-1,5-imino-L-fucitol (2)

A mixture of **14a** (23 mg, 0.045 mmol) in MeOH (3 mL) was added 0.2 mL 6 N HCl and 10% Pd-C (5 mg). The mixture was stirred for 24 h under H_2 atmosphere. The catalyst was then removed by filtration through Celite, and the filtrate was concentrated. The residue was dissolved in 1.0 M methanolic solution of HCl (1.0 mL) and the solvent was evaporated. The residue, dissolved in H_2O, was introduced to a Dowex-50 W-X8-100 (H^+) packed ion-exchange column (pre-washed with MeOH and H_2O), washed with water (100 mL) and MeOH (50 mL) and then the product was eluted with 1.0 M aqueous solution of NH_4OH. The combined pure fractions were evaporated *in vacuo* to give **2** (6.5 mg, 91%) as a white solid after lyophilization. The NMR data of the free amine **2** were in excellent agreement to those reported in literature; [28,35] $[\alpha]_D^{20}$ −42.4 (*c* 0.48, MeOH); ^{1}H NMR (500 MHz, D_2O) δ 3.70–3.51 (m, 2H, H_4 & H_2), 3.30 (d, J = 9.4 Hz, 1H, H_3), 2.97 (d, J = 8.4 Hz, 1H, $H_{1\text{-eq}}$), 2.78 (m, 1H, H_5), 2.30 (t, J = 11.4 Hz, 1H, $H_{1\text{-ax}}$), 0.94 (d, J = 6.6 Hz, 3H, CH_3). ^{13}C NMR (125 MHz, D_2O) δ 75.65 (C_3), 72.99 (C_4), 68.06 (C_2), 54.45 (C_5), 49.19 (C_1), 16.70 (C_6). HRMS: Calcd for $C_6H_{14}NO_3$, $[M + H]^+$, 148.0974; Found, 148.0971.

4.2.12. N-(4-Hydroxybutyl)- 1,5-dideoxy-l,5-imino-L-fucitol (22)

A mixture of **14a** (23.0 mg, 0.045 mmol) and 10% Pd-C (10.0 mg) in HOAc (0.25 mL), H_2O (0.5 mL), and THF (1.0 mL) was stirred for 24 h under H_2 atmosphere. The catalyst was then removed by filtration through Celite, and the filtrate was concentrated. The residue was dissolved in 1.0 M methanolic solution of HCl (1.0 mL) and the solvent was evaporated. The residue, dissolved in H_2O, was introduced to a Dowex-50 W-X8-100 (H^+) packed ion-exchange column (pre-washed with MeOH and H_2O), washed with water (100 mL) and MeOH (50 mL) and then the product was eluted with 1.0 M aqueous solution of NH_4OH. The combined pure fractions were evaporated *in vacuo* to give **22** (8.5 mg, 85%) as a white powder after lyophilization. ^{1}H NMR (500 MHz, CD_3OD) δ 3.88 (td, J = 10.0, 4.9 Hz, 1H, H_2), 3.73 (d, J = 1.5 Hz, 1H, H_4), 3.70–3.57 (m, 2H, CH_2OH), 3.33 (dd, J = 9.3, 3.3 Hz, 1H, H_3), 3.14 (dd, J = 11.3, 4.9 Hz, 1H, $H_{1\text{-eq}}$), 2.91–2.78 (m, 1H, 1x NC*H*HCH$_2$), 2.70–2.53 (m, 2H, 1x NC*H*HCH$_2$ & H_5), 2.25 (t, J = 10.7 Hz, 1H, $H_{1\text{-ax}}$), 1.71–1.62 (m, 2H, 1x NCH_2CH_2), 1.62–1.54 (m, 2H, CH_2), 1.30 (d, J = 6.6 Hz, 3H, CH_3). ^{13}C NMR (125 MHz, CD_3OD) δ 77.06 (C_3), 74.59 (C_4), 68.73 (C_2), 62.65 (CH_2OH), 60.20 (C_5), 57.33 (C_1), 53.79 (NCH_2), 31.53 (CH_2), 21.81 (CH_2), 16.05 (CH_3, C_6). HRMS: Calcd for $C_{10}H_{22}NO_4$, $[M + H]^+$, 220.1549; Found, 220.1544.

4.2.13. N-Decyl-1,5-Dideoxy-1,5-imino-L-fucitol (16)

Compound **16** was prepared from **14b** as described in the preparation of **2**, yielding **16** (90%) as a solid after lyophilization; ^{1}H NMR (500 MHz, CD_3OD) δ 3.80 (td, J = 9.4, 4.9 Hz, 1H, H_2), 3.65 (dd, J = 3.3, 1.4 Hz, 1H, H_4), 3.25 (dd, J = 9.4, 3.3 Hz, 1H, H_3), 3.01 (dd, J = 11.2, 4.9 Hz, 1H, $H_{1\text{-eq}}$), 2.77–2.63 (m, 1H, NC*H*H), 2.57–2.39 (m, 2H, H_5 & NC*H*H), 2.14 (t, J = 10.8 Hz, 1H, $H_{1\text{-ax}}$), 1.49 (m, 2H, C*H*2), 1.39–1.24 (m, 14H, 7 × CH_2), 1.21 (d, J = 6.6 Hz, CH_3, H_6), 0.91 (t, J = 7.0 Hz, 3H, $CHCH_3$). ^{13}C NMR (125 MHz, CD_3OD) δ 77.31(C_3), 74.84 (C_4), 69.02 (C_2), 59.77 (C_5), 57.74 (C_1), 53.96 (NCH_2CH_2), 33.03, 30.70, 30.66, 30.60, 30.42, 28.58, 24.65, 23.70 (each CH_2), 16.32(C_6), 14.41(CH_3). HRMS: Calcd for $C_{16}H_{34}NO_3$, $[M + H]^+$, 288.2539; Found, 288.2539.

4.2.14. N-Octyl-1,5-dideoxy-1,5-imino-L-fucitol (17)

Compound **17** was prepared from **14c** as described in the preparation of **2**, yielding **17** (85%) as a solid after lyophilization; ^{1}H NMR (500 MHz, CD_3OD) δ 3.83 (td, J = 9.9, 4.9 Hz, 1H, H_2), 3.69 (d, J = 3.0 Hz,1H, H_4), 3.29 (dd, J = 9.3, 3.0 Hz, 1H, H_3), 3.07 (dd, J = 11.0, 4.8 Hz, 1H, $H_{1\text{-eq}}$), 2.85–2.71 (m, 1H, NC*H*H), 2.70–2.52 (m, 2H, H_5 & NCH*H*), 2.26 (t, J = 10.5 Hz, 1H, $H_{1\text{-ax}}$), 1.53 (m, 2H), 1.32 (m, 10*H*), 1.24 (d, J = 6.6 Hz, 3H, CH_3), 0.91 (t, J = 6.9 Hz, 3H, CH_3). ^{13}C NMR (125 MHz, CD_3OD) δ 76.92 (C_3), 74.42 (C_4), 68.62 (C_2), 60.11 (C_5), 57.21 (C_1), 53.97 (NCH_2), 32.95, 30.51, 30.35, 28.45, 24.46, 23.68 (each CH_2), 15.95 (C_6), 14.39 (CH_3). HRMS: Calcd for $C_{14}H_{30}NO_3$, $[M + H]^+$, 260.2226; Found, 260.2232.

4.2.15. N-Butyl-1,5-dideoxy-1,5-imino-L-fucitol (18)

Compound **18** was prepared from **14d** as described in the preparation of **2**, yielding **18** (88%) as a solid after lyophilization; ^{1}H NMR (500 MHz, D_2O) δ 4.13–4.18(m, 1H, H_2), 4.11(s, 1H, H_4), 3.72 (d, J = 9.5, 1H, H_3), 3.52–3.60 (m, 2H, $H_{1\text{-eq}}$ & H_5), 3.30 (dt, J = 12.0, 5.5 Hz, 1H, NC*H*H), 3.20 (dt, J = 12.0, 5.5 Hz, 1H, NC*H*H) 3.03 (t, J = 12.0 Hz, 1H, $H_{1\text{-ax}}$) 1.73–1.81 (m, 2H, CH_2), 1.48 (d, J = 7.0, 3H, CH_3), 1.42–1.49 (m, 2H, CH_2), 1.02 (t, J = 7.5, 3H, CH_3); ^{13}C NMR (125 MHz, D_2O) δ 75.48 (C_3), 73.71 (C_4), 67.40 (C_2), 63.15 (C_5), 55.90 (C_1), 55.14 (NCH_2), 26.09 (CH_2), 21.86 (CH_2), 15.99 (CH_3, C_6), 15.33 (CH_3). HRMS: Calcd for $C_{10}H_{21}NO_3$, $[M + H]^+$, 204.1600; Found, 204.1604.

4.2.16. N-(2-Hydroxyethyl)-1,5-dideoxy-l,5-imino-L-fucitol (19)

Compound **19** was prepared from **14e** as described in the preparation of **2**, yielding **19** (78%) as a solid after lyophilization; ^{1}H NMR (500 MHz, D_2O) δ 3.85 (m, 4H, H_2 & H_4 & CH_2OH), 3.51 (d, J = 9.7 Hz, 1H, H_3), 3.28–3.15 (m, 1H, $H_{1\text{-eq}}$), 3.07–2.93 (m, 1H, NC*H*HCH$_2$), 2.82–2.63 (m, 2H, H_5 & NC*H*HCH$_2$), 2.36 (t, J = 10.7 Hz, 1H, $H_{1\text{-ax}}$), 1.13 (d, J = 6.4 Hz, 3H, CH_3). ^{13}C NMR (125 MHz, D_2O) δ 74.91(C_3), 73.13 (C_4), 66.94 (C_2), 58.49 (C_5), 57.51 (CH_2OH), 56.07 (C_1), 53.16 (NCH_2), 15.24 (C_6). HRMS: Calcd for $C_8H_8NO_4$, $[M + H]^+$, 192.1236; Found, 192.1228.

4.2.17. N-Adamantylcarbonylaminoethyl-1,5-Dideoxy-1,5-imino-L-fucitol (20)

Compound **20** was prepared from **15** as described in the preparation of **2**, yielding **20** (83%) as solids after lyophilization; ^{1}H NMR (500 MHz, CD_3OD) δ 3.98 (ddd, J = 14.2, 9.5, 4.4 Hz, 1H, H_2), 3.85 (m, 1H, H_4), 3.49 (dd, J = 10.5, 6.0 Hz, 2H, NCH_2), 3.45 (dd, J = 9.1, 2.4 Hz, 1H, H_3), 3.39 (dd, J = 11.9, 4.9 Hz, 1H, $H_{1\text{-eq}}$), 3.29–3.22 (m, 1H, H_5), 3.22–3.17 (m, 1H, C*H*HNH), 3.08–3.00 (m, 1H, C*H*HNH), 2.76 (t, J = 11.2 Hz, 1H, $H_{1\text{-ax}}$), 2.04 (s, 3H, 3 × C*H*CH$_2$), 1.88 (d, J = 2.4 Hz, 6H, 3 × CHCH_2), 1.78 (m, 6H, 3x CHCH_2), 1.39 (d, J = 6.6 Hz, 3H, CH_3). ^{13}C NMR (125 MHz, CD_3OD) δ 180.88 (C═O), 74.11 (C_3), 71.60 (C_4), 65.74(C_2), 60.60 (C_5), 55.23(C_1), 52.55 (CH_2), 40.42(C), 38.85, 38.70, 36.18, 36.11, 34.68 (each CH_2), 28.17(CH), 13.43 (C_6, CH_3); HRMS: Calcd for $C_{19}H_{33}N_2O_4$, $[M + H]^+$, 353.2440; Found, 353.2451.

4.2.18. 1,5,6-Trideoxy-1,5-imino-D-altritol (5)

Compound **5** was prepared from **9** as described in the preparation of **2**, yielding **5** (93%) or prepared from **11** in 83% yield, as solids after lyophilization. $[\alpha]_D^{20}$ 0.9 (*c* 0.55, MeOH) [lit. $[\alpha]_D^{20}$ 2 (*c* 1.1, MeOH)]; ^{1}H NMR (500 MHz, D_2O) δ 3.93–3.78 (m, 2H, H_2 & H_3), 3.55 (d, J = 8.9 Hz, 1H, H_4), 2.93 (m, 2H, $H_{1\text{-eq}}$ & H_5), 2.76 (dd, J = 14.0, 2.4 Hz, 1H, $H_{1\text{-ax}}$), 1.35 (d, J = 6.6, 3H, CH_3). ^{13}C NMR (125 MHz, D_2O) δ 70.82 (C_3), 69.96 (C_4), 68.67 (C_2), 50.49 (C_5), 44.23 (C_1), 15.86 (C_6). HRMS: Calcd for $C_6H_{14}NO_3$, $[M + H]^+$, 148.0974; Found, 148.0967.

4.3. Fucosidase inhibition assays

The substrate used for the enzyme assays was 4-nitrophenyl α-L-fucopyranoside. Substrate solutions were made from a stock solution (10 mM) in 10 mL batches, as required, by dissolving the appropriate mass of substrate in the correct buffer solution for the enzyme. These were kept at 4 °C when not in use. Assays were carried out in triplicate, using water as a blank in place of the inhibitor. The concentrations of the enzyme were adjusted so that the reading for the final absorbance was in the range of 1.0–2.0 units over a reaction time of 20 min. Linearity over the time course of the reaction was checked using a series of incubation times. The following were combined in the well of a flat-bottomed 96-well (300 μL) microtitre plate:10 μL of enzyme solution; 10 μL inhibitor solution; 80 μL substrate solution. The reaction mix was incubated at 25 °C for 20 min and was quenched by the addition of 100 μL of 2 M Na_2CO_3. Absorbance at 405 nm was measured immediately using a microtitre plate reader. Percentage inhibition was plotted against the log of the inhibitor concentration and a trendline was fitted using Microsoft Excel. The IC_{50} value for each compound calculated from the value of the log of the inhibitor concentration at 50% inhibition of enzyme activity.

4.4. Molecular modelling

The PDB for fucosidase of *T. maritima* was available from the RCSB-PDB, while for the fucosidase of *B. taurus*, a homology model was constructed. The sequence for the *B. taurus* fucosidase (Accession: AAI12589.1 GI: 86827599) was obtained from NCBI (National Center for Biotechnology Information). Next a BlastP search along with the BLOSSUM62 substitution matrix, generated putative template PDBs with the minimum identity of 35% and 87% sequence coverage, provided in Table S1, in supplementary information. Later, homology modelling on templates having more than 35% identity and at least 85% of coverage of the query sequence was conducted. The software programme MOE 2018.01 implementing the Amber 99 forcefield was used [65]. After generated homology models were assessed. Initially, the generated homology model and the template were superimposed giving an RMSD difference, which was less than 1 Å [66]. See Fig. S1 in the supplementary information. The Z-score for the templates and homology models, was assessed using ProSA, a protein structure analysis tool, respectively ([67]. See Fig. S2 in supplementary information. Next, the Ramachandran plot was generated. In the Ramachandran plot, the core or the allowed regions are those satisfying the Ψ/φ angle pairs for residues in a protein. See Fig. S4 in supplementary information [68,69]. For those amino acids which did not comply with the requirements of the Ramachandran plot, further energy minimization was done. ERRAT plots, which are for the determination of errors in model building were performed. See Fig. S3 in the supplementary information) [70]. Verify 3D was used to determine the compatibility of the constructed homology model (3D) with its own amino acid sequence (1D) by assigning a structural class based on its location and environment (alpha, beta, loop, polar, nonpolar, etc.); a score of > 80% was considered acceptable (Fig. 4) [71]. The active site for docking was identified with the active site finder tool of MOE and later, the docked pose of the largest ensembled cluster within a RMSD of 2 Å, was selected [72]. The triangle matcher placement method and GBVI/WSA dG scoring was used for the docking. Molecular dynamics (MD) was performed on the selected docked poses of compounds, **2** and **16** [57]. This analysis was carried out also using MOE 2018.01 software [65]. Partial charges were calculated and energy minimizations were done. MD was carried for a duration of 100 ps. The adopted docking procedure was validated using the co-crystallized structure of iso-6FNJ binding to fucosidase was obtained from the PDB (2ZXD). After docking iso-6FNJ to the fucosidase, an RMSD value of 0.391 Å between the co-crystallized structure and the docked structure indicated that the adopted docking procedure was reliable [73].

4.5. Cell culture and cytotoxicity evaluation

4.5.1. Materials and cell lines

The MCF-7 breast cancer and DU-145 prostate cancer cell lines were obtained from Dr. Stephen Rea, National University of Ireland, Galway. The BT-474 breast cancer cell line was obtained from Dr. Helen Dodson, National University of Ireland, Galway.

MCF-7 were cultured in Dulbecco's modified Eagle's medium (DMEM) containing high glucose (4.5 g/mL) and supplemented with 1% penicillin-streptomycin and 10% heat-inactivated fetal bovine serum (FBS). DU-145 were cultured in RPMI-1640 medium and supplemented with 1% 2 mM L-glutamine, 1% penicillin-streptomycin and 10% non heat-inactivated fetal bovine serum (FBS). BT-474 were cultured in Dulbecco's modified Eagle's medium (DMEM)/Nutrient mixture F-12 Ham and supplemented with 1% penicillin-streptomycin and 10% non heat-inactivated fetal bovine serum (FBS). All cells grew as adherent cultures. Cell culture reagents were obtained from Sigma-Aldrich. Disposable sterile plasticware was obtained from Sarstedt (Numbrecht, Germany).

4.5.2. Cytotoxicity measurements using the MTT assay

The MTT colorimetric assay was used to determine cell viability. Cells were added to 96-well plates at a cell density of 1000 cells per well (MCF-7, 200 μL per well), 2000 cells per well (DU-145, 200 μL per well) and 3000 cells per well (BT-474, 200 μL per well) and allowed to adhere over 24 h. Compound solutions in DMSO were added after 24 h (1% v/v final concentration in well). The control cells were exposed to the same concentration of the vehicle control alone (DMSO). All cells were incubated at 37 °C and 5% CO_2 (humidified atmosphere) for 72 h. MTT (20 μL, 5 mg/mL solution) was added after 72 h and the cells were incubated for a further 3 h. The supernatant was then removed using a multi-transfer pipette and DMSO (100 μL) added to dissolve the MTT formazan crystals. The absorbance was determined using a plate reader at 550 nm with a reference at 690 nm. Cell viability is expressed as a percentage of the vehicle-only treated control (DMSO). Dose-response curves were analyzed by non-linear regression analysis and IC_{50} values were determined using GraphPad Prism software, v 8.0 (GraphPad Inc., San Diego, CA, USA). The *in vitro* activity of the drugs towards all cell lines is expressed as IC_{50} (i.e. concentration required for the reduction of the mean cell viability to 50%).

4.6. Tumor cell proliferation assay using HNO41, HNO97, HNO210 & NCH644 cell lines

To further assess the influence of **16** on tumor cell proliferation well-characterized human head and neck carcinoma cell lines (HNO41, HNO97, HNO210; [74–76] as well as glioblastoma-initiating cells (NCH644, [62]) were incubated with increasing concentrations (0.015 μM - 45 μM) of 16 for 72 h. Cells were grown either in media containing 10% fetal calf serum (HNO41, HNO97, HNO210) or under serum free conditions as described before [71–73]. Each concentration was measured in four technical replicates with the CellTiter-Glo® 3D Cell Viability Assay. After adding the CellTiter-Glo substrate the plate was shaken for 5 min and afterwards incubated for 30 min to get a stable luminescence signal. This was measured as relative light units by a Tecan Infinite F200 Pro. IC50 was determined by a sigmoidal fit in version 5 of the GraphPad Prism software.

Acknowledgement

Research presented herein was supported by Science Foundation Ireland (07/IN.1/B966), the Irish Research Council (GOI PhD Scholarships to JZ, AN) and the European Commission through COST Action CM1106. The authors thank Guan-Nan Wang for recording NMR spectra and to Nadine Martinet for organization of the COST Action CM1106 screening library that led to identification of the activity for

16. The authors thank Dr. Stephen Rea and Dr. Helen Dodson for gifts of tumour cells.

Appendix A. Supplementary material

Supplementary data to this article can be found online at https://doi.org/10.1016/j.bioorg.2018.12.003.

References

[1] C.H. Wong, D.P. Dumas, Y. Ichikawa, K. Koseki, S.J. Danishefsky, B.W. Weston, J.B. Lowe, Specificity, inhibition, and synthetic utility of a recombinant human alpha-1,3-fucosyl-transferase, J. Am. Chem. Soc. 114 (1992) 7321–7322.

[2] P. Compain, O.R. Martin, Design, synthesis and biological evaluation of iminosugar-based glycosyltransferase inhibitors, Curr. Top. Med. Chem. 3 (2003) 541–560.

[3] L. Somsak, V. Nagy, Z. Hadady, T. Docsa, P. Gergely, Glucose analog inhibitors of glycogen phosphorylases as potential antidiabetic agents: recent developments, Curr. Pharm. Des. 9 (2003) 1177–1189.

[4] V.L. Schramm, P.C. Tyler, Imino-sugar-based nucleosides, Curr. Top. Med. Chem. 3 (2003) 525–540.

[5] R.E. Lee, M.D. Smith, L. Pickering, G.W.J. Fleet, An approach to combinatorial library generation of galactofuranose mimics as potential inhibitors of mycobacterial cell wall biosynthesis: Synthesis of a peptidomimetic of uridine 5 '-diphosphogalactofuranose (UDP-Galf), Tetrahedron Lett. 40 (1999) 8689–8692.

[6] R.E. Lee, M.D. Smith, R.J. Nash, R.C. Griffiths, M. McNeil, R.K. Grewal, W.X. Yan, G.S. Besra, P.J. Brennan, G.W.J. Fleet, Inhibition of UDP-Gal mutase and mycobacterial galactan biosynthesis by pyrrolidine analogues of galactofuranose, Tetrahedron Lett. 38 (1997) 6733–6736.

[7] H. Moriyama, T. Tsukida, Y. Inoue, K. Yokota, K. Yoshino, H. Kondo, N. Miura, S. Nishimura, Azasugar-based MMP/ADAM inhibitors as antipsoriatic agents, J. Med. Chem. 47 (2004) 1930–1938.

[8] A.E. Stütz, Iminosugars as Glycosidase Inhibitors: Nojirimycin and Beyond, Wiley-VCH, Weinheim, 1999.

[9] P. Sears, C.H. Wong, Carbohydrate mimetics: a new strategy for tackling the problem of carbohydrate-mediated biological recognition, Angew. Chem. Int. Ed. 38 (1999) 2301–2324.

[10] T.M. Gloster, G.J. Davies, Glycosidase inhibition: assessing mimicry of the transition state, Org. Biomol. Chem. 8 (2010) 305–320.

[11] V.H. Lillelund, H.H. Jensen, X.F. Liang, M. Bols, Recent developments of transition-state analogue glycosidase inhibitors of non-natural product origin, Chem. Rev. 102 (2002) 515–553.

[12] O.R. Martin, P. Compain, Iminosugars: Recent insights into their bioactivity and potential as therapeutic agents – preface, Curr. Top. Med. Chem. 3 (2003).

[13] D.J. Becker, J.B. Lowe, Fucose: biosynthesis and biological function in mammals, Glycobiology 13 (2003) 41r–53r.

[14] E. Staudacher, alpha 1,3-fucosyltransferases, Trends Glycosci. Glycotechnol. 8 (1996) 391–408.

[15] D.H. Dube, C.R. Bertozzi, Glycans in cancer and inflammation. Potential for therapeutics and diagnostics, Nat. Rev. Drug Discov. 4 (2005) 477–488.

[16] D. Ayude, J. Fernandez-Rodriguez, F.J. Rodriguez-Berrocal, V.S. Martinez-Zorzano, A. de Carlos, E. Gil, M.P. de la Cadena, Value of the serum alpha-L-fucosidase activity in the diagnosis of colorectal cancer, Oncology 59 (2000) 310–316.

[17] K. Yuan, C.M. Listinsky, R.K. Singh, J.J. Listinsky, G.P. Siegal, Cell surface associated alpha-L-fucose moieties modulate human breast cancer neoplastic progression, Pathol. Oncol. Res. 14 (2008) 145–156.

[18] M.C. Glick, V.A. Kothari, A.H. Liu, L.I. Stoykova, T.F. Scanlin, Activity of fucosyltransferases and altered glycosylation in cystic fibrosis airway epithelial cells, Biochimie 83 (2001) 743–747.

[19] S.D. Szajda, A. Jankowska, K. Zwierz, Carbohydrate markers in colon carcinoma, Dis. Markers 25 (2008) 233–242.

[20] Z.J. Tu, Y.N. Lin, C.H. Lin, Development of fucosyltransferase and fucosidase inhibitors, Chem. Soc. Rev. 42 (2013) 4459–4475.

[21] M. Dubernet, A. Defoin, C. Tarnus, Asymmetric synthesis of the l-fuco-nojirimycin, a nanomolar α-l-fucosidase inhibitor, Bioorg. Med. Chem. Lett. 16 (2006) 1172–1174.

[22] N. Asano, K. Yasuda, H. Kizu, A. Kato, J.Q. Fan, R.J. Nash, G.W. Fleet, R.J. Molyneux, Novel α-L-fucosidase inhibitors from the bark of *Angylocalyx pynaertii* (Leguminosae), FEBS J. 268 (2001) 35–41.

[23] Y. Zhao, W. Liu, Y. Zhou, X. Zhang, P.V. Murphy, N-(8-(3-ethynylphenoxy) octyl-1-deoxynojirimycin suppresses growth and migration of human lung cancer cells, Bioorg. Med. Chem. Lett. 20 (2010) 7540–7543.

[24] Y. Zhao, Y. Zhou, K.M. O'Boyle, P.V. Murphy, Biological study of the angiogenesis inhibitor N-(8-(3-ethynylphenoxy) octyl-1-deoxynojirimycin, Chem. Biol. Drug Des. 75 (2010) 570–577.

[25] Y. Zhao, Y. Zhou, K.M. O'Boyle, P.V. Murphy, Hybrids of 1-deoxynojirimycin and aryl-1, 2, 3-triazoles and biological studies related to angiogenesis, Bioorgan. Med. Chem. 16 (2008) 6333–6337.

[26] A. Mitrakou, N. Tountas, A. Raptis, R. Bauer, H. Schulz, S. Raptis, Long-term effectiveness of a new α-glucosidase inhibitor (BAY m1099-miglitol) in insulin-treated Type 2 diabetes mellitus, Diabet. Med. 15 (1998) 657–660.

[27] L. Yu, K. Ikeda, A. Kato, I. Adachi, G. Godin, P. Compain, O. Martin, N. Asano, α-1-C-Octyl-1-deoxynojirimycin as a pharmacological chaperone for Gaucher disease, Bioorgan. Med. Chem. 14 (2006) 7736–7744.

[28] G. Godin, P. Compain, O.R. Martin, K. Ikeda, L. Yu, N. Asano, α-1-C-Alkyl-1-deoxynojirimycin derivatives as potent and selective inhibitors of intestinal isomaltase: remarkable effect of the alkyl chain length on glycosidase inhibitory profile, Bioorg. Med. Chem. Lett. 14 (2004) 5991–5995.

[29] G.-N. Wang, G. Reinkensmeier, S.-W. Zhang, J. Zhou, L.-R. Zhang, L.-H. Zhang, T.D. Butters, X.-S. Ye, Rational design and synthesis of highly potent pharmacological chaperones for treatment of N370S mutant Gaucher disease, J. Med. Chem. 52 (2009) 3146–3149.

[30] T.D. Butters, Gaucher disease, Curr. Opin. Chem. Biol. 11 (2007) 412–418.

[31] C. Porto, M. Cardone, F. Fontana, B. Rossi, M.R. Tuzzi, A. Tarallo, M.V. Barone, G. Andria, G. Parenti, The pharmacological chaperone N-butyldeoxynojirimycin enhances enzyme replacement therapy in Pompe disease fibroblasts, Mol. Ther. 17 (2009) 964–971.

[32] Z. Yu, A.R. Sawkar, L.J. Whalen, C.-H. Wong, J.W. Kelly, Isofagomine-and 2, 5-anhydro-2, 5-imino-D-glucitol-based glucocerebrosidase pharmacological chaperones for Gaucher disease intervention, J. Med. Chem. 50 (2007) 94–100.

[33] T. Wennekes, R.J. van den Berg, W. Donker, G.A. van der Marel, A. Strijland, J.M. Aerts, H.S. Overkleeft, Development of adamantan-1-yl-methoxy-functionalized 1-deoxynojirimycin derivatives as selective inhibitors of glucosylceramide metabolism in man, J. Organ. Chem. 72 (2007) 1088–1097.

[34] C.-W. Ho, Y.-N. Lin, C.-F. Chang, S.-T. Li, Y.-T. Wu, C.-Y. Wu, C.-F. Chang, S.-W. Liu, Y.-K. Li, C.-H. Lin, Discovery of different types of inhibition between the human and *Thermotoga maritima* α-Fucosidases by fuconojirimycin-based derivatives, Biochemistry 45 (2006) 5695–5702.

[35] I. Jefferies, B.R. Bowen, Synthesis of inhibitors of α-1, 3-fucosyltransferase, Bioorg. Med. Chem. Lett. 7 (1997) 1171–1174.

[36] G.W. Fleet, A. Karpas, R.A. Dwek, L.E. Fellows, A. Tyms, S. Petursson, S.K. Namgoong, N.G. Ramsden, P.W. Smith, J.C. Son, Inhibition of HIV replication by amino-sugar derivatives, FEBS Lett. 237 (1988) 128–132.

[37] A. Peer, A. Vasella, Synthesis of an L-fucose-derived cyclic nitrone and its conversion to α-L-fucosidase Inhibitors, Helv. Chim. Acta 82 (1999) 1044–1065.

[38] H. Paulsen, M. Matzke, B. Orthen, R. Nuck, W. Reutter, Monosaccharide mit stickstoff im ring, XXXIX. Synthese von modifizierten α-L-fucosidase-inhibitoren, die 1,5-didesoxy-1,5-imino-L-fucit als Basisstruktur enthalten, Eur. J. Org. Chem. (1990, 1990,) 953–963.

[39] N. Chida, M. Ohtsuka, S. Ogawa, Synthesis of 2-acetoxy-4-formylphenyl 2,3-Di-O-acetyl-6-deoxy-beta-D-arabino-5-hexulofuranoside, structure confirmation of the anomeric configuration of antibiotic hygromycin-A, Chem. Lett. (1988) 969–972.

[40] N. Chida, M. Ohtsuka, K. Nakazawa, S. Ogawa, Total synthesis of antibiotic hygromycin-A, J. Org. Chem. 56 (1991) 2976–2983.

[41] G.W.J. Fleet, A.N. Shaw, S.V. Evans, S.V. Evans, Synthesis from D-Glucose of 1,5-Dideoxy-1,5-Imino-L-Fucitol, a Potent Alpha-L-Fucosidase Inhibitor, J. Chem. Soc. Chem. Commun. (1985) 841–842.

[42] E.W. Baxter, A.B. Reitz, Expeditious Synthesis of Azasugars by the Double Reductive Amination of Dicarbonyl Sugars, J Org Chem 59 (1994) 3175–3185.

[43] A.F. AbdelMagid, K.G. Carson, B.D. Harris, C.A. Maryanoff, R.D. Shah, Reductive amination of aldehydes and ketones with sodium triacetoxyborohydride. Studies on direct and indirect reductive amination procedures, J. Org. Chem. 61 (1996) 3849–3862.

[44] K.I. Fujita, T. Fujii, R. Yamaguchi, Cp*Ir complex-catalyzed N-heterocyclization of primary amines with diols: a new catalytic system for environmentally benign synthesis of cyclic amines, Org. Lett. 6 (2004) 3525–3528.

[45] C. Cimarelli, G. Palmieri, Asymmetric reduction of enantiopure imines with zinc borohydride: stereoselective synthesis of chiral amines, Tetrahedron-Asymmetry 11 (2000) 2555–2563.

[46] Z.Q. Yu, A.R. Sawkar, L.J. Whalen, C.H. Wong, J.W. Kelly, Isofagomine- and 2,5-anhydro-2,5-imino-D-glucitol-based glucocerebrosidase pharmacological chaperones for Gaucher disease intervention, J. Med. Chem. 50 (2007) 94–100.

[47] J. Zhou, Y. Zhang, X. Zhou, J. Zhou, L.H. Zhang, X.S. Ye, X.L. Zhang, An expeditious one-pot synthesis of 1,6-dideoxy-N-alkylated nojirimycin derivatives and their inhibitory effects on the secretion of IFN-gamma and IL-4, Bioorg. Med. Chem. 16 (2008) 1605–1612.

[48] F. Peri, F. Granucci, B. Costa, I. Zanoni, C. Marinzi, F. Nicotra, Inhibition of lipid A stimulated activation of human dendritic cells and macrophages by amino and hydroxylamino monosaccharides, Angew. Chem. Int. Ed. 46 (2007) 3308–3312.

[49] R. Polt, D. Sames, J. Chruma, Glycosidase inhibitors: synthesis of enantiomerically pure aza-sugars from Schiff base amino esters via tandem reduction-alkenylation and osmylation, J. Org. Chem. 64 (1999) 6147–6158.

[50] J. Streith, A. Boiron, T. Sifferlen, C. Strehler, T. Tschamber, A simple asymmetric-synthesis of 2-substituted 2,3-dihydro-4-pyridones, Tetrahedron Lett. 35 (1994) 3927–3930.

[51] J. Streith, A. Boiron, J.L. Paillaud, E.M. Rodriguezperez, C. Strehler, T. Tschamber, M. Zehnder, Chelate-controlled asymmetric-synthesis of 2-substituted 2,3-dihydropyridin-4(1h)-ones – synthesis of D-aminodeoxyaltrose and L-aminodeoxyaltrose derivatives, Helv. Chim. Acta 78 (1995) 61–72.

[52] G. Sulzenbacher, C. Bignon, T. Nishimura, C.A. Tarling, S.G. Withers, B. Henrissat, Y. Bourne, Crystal structure of *Thermotoga maritima* alpha-L-fucosidase – insights into the catalytic mechanism and the molecular basis for fucosidosis, J. Biol. Chem. 279 (2004) 13119–13128.

[53] S. Ogawa, M. Mori, G. Takeuchi, F. Doi, M. Watanabe, Y. Sakata, Convenient synthesis and evaluation of enzyme inhibitory activity of several N-alkyl-, N-phenylalkyl, and cyclic isourea derivatives of 5a-Carba-alpha-DL-fucopyranosylamine, Bioorg. Med. Chem. Lett. 12 (2002) 2811–2814.

[54] C.A. Lipinski, F. Lombardo, B.W. Dominy, P.J. Feeney, Experimental and computational approaches to estimate solubility and permeability in drug discovery and development settings1, Adv. Drug Deliv. Rev. 46 (2001) 3–26.

[55] M.D. Shultz, Setting expectations in molecular optimizations: strengths and limitations of commonly used composite parameters, Bioorg. Med. Chem. Lett. 23 (2013) 5980–5991.
[56] H.J. Wu, C.W. Ho, T.P. Ko, S.D. Popat, C.H. Lin, A.H.J. Wang, Structural basis of α-fucosidase inhibition by iminocyclitols with Ki values in the micro-to picomolar range, Angew. Chem. Int. Ed. 49 (2010) 337–340.
[57] R.Z. Batran, D.H. Dawood, S.A. El-Seginy, T.J. Maher, K.S. Gugnani, A.N. Rondon-Ortiz, Coumarinyl pyranopyrimidines as new neuropeptide S receptor antagonists; design, synthesis, homology and molecular docking, Bioorg. Chem. 75 (2017) 274–290.
[58] P.S. Kharkar, S. Warrier, R.S. Gaud, Reverse docking: a powerful tool for drug repositioning and drug rescue, Future Med. Chem. 6 (2014) 333–342.
[59] P.K. Singh, A. Negi, P.K. Gupta, M. Chauhan, R. Kumar, Toxicophore exploration as a screening technology for drug design and discovery: techniques, scope and limitations, Arch. Toxicol. 90 (2016) 1785–1802.
[60] A. Negi, N. Bhandari, B.R.K. Shyamlal, S. Chaudhary, Inverse docking based screening and identification of protein targets for Cassiarin alkaloids against *Plasmodium falciparum*, Saudi Pharmaceut. J. 26 (2018) 546–567.
[61] A. Negi, J. Zhou, S. Sweeney, P.V. Murphy, Ligand design for somatostatin receptor isoforms 4 and 5, Eur. J. Med. Chem. 163 (2019) 149–159.
[62] B. Campos, Z. Gal, A. Baader, T. Schneider, C. Sliwinski, K. Gassel, J. Bageritz, N. Grabe, A. von Deimling, P. Beckhove, Aberrant self-renewal and quiescence contribute to the aggressiveness of glioblastoma, J. Pathol. 234 (2014) 23–33.
[63] S.-Y. Huang, S.Z. Grinter, X. Zou, Scoring functions and their evaluation methods for protein–ligand docking: recent advances and future directions, Phys. Chem. Chem. Phys. 12 (2010) 12899–12908.
[64] R.J. Molenaar, J.P. Maciejewski, J.W. Wilmink, C.J. Noorden, Wild-type and mutated IDH1/2 enzymes and therapy responses, Oncogene 37 (2018) 949–1960.
[65] Chemical Computing Group ULC, Molecular Operating Environment (MOE), 2018. 01, 2018.
[66] A. Negi, S. Bhushan, P. Gupta, P. Garg, R. Kumar, Cystathionine β-lyase-like protein with pyridoxal binding domain characterized in Leishmania major by comparative sequence analysis and homology modelling, ISRN Comput. Biol. 2013 (2013) 1–9.
[67] M. Wiederstein, M.J. Sippl, ProSA-web: interactive web service for the recognition of errors in three-dimensional structures of proteins, Nucl. Acids Res. 35 (2007) W407–W410.
[68] R.A. Laskowski, M.W. MacArthur, D.S. Moss, J.M. Thornton, PROCHECK: a program to check the stereochemical quality of protein structures, J. Appl. Crystallogr. 26 (1993) 283–291.
[69] G.N. Ramachandran, C. Ramakrishnan, V. Sasisekharan, Stereochemistry of polypeptide chain configurations, J. Mol. Biol. 7 (1963) 95–99.
[70] C. Colovos, T.O. Yeates, Verification of protein structures: patterns of nonbonded atomic interactions, Protein Sci. 2 (1993) 1511–1519.
[71] R. Lüthy, J.U. Bowie, D. Eisenberg, Assessment of protein models with three-dimensional profiles, Nature 356 (1992) 83–85.
[72] J. Zhou, M. Reidy, C. O'Reilly, D.V. Jarikote, A. Negi, A. Samali, E. Szegezdi, P.V. Murphy, Decorated macrocycles via ring-closing double-reductive amination. Identification of an apoptosis inducer of leukemic cells that at least partially antagonizes a 5-HT2 receptor, Org. Lett. 17 (2015) 1672–1675.
[73] M. Chauhan, A. Rana, J.M. Alex, A. Negi, S. Singh, R. Kumar, Design, microwave-mediated synthesis and biological evaluation of novel 4-aryl (alkyl) amino-3-nitroquinoline and 2,4-diaryl (dialkyl) amino-3-nitroquinolines as anticancer agents, Bioorg. Chem. 58 (2015) 1–10.
[74] S. Ninck, C. Reisser, G. Dyckhoff, B. Helmke, H. Bauer, C. Herold-Mende, Expression profiles of angiogenic growth factors in squamous cell carcinomas of the head and neck, Int. J. Cancer 106 (2003) 34–44.
[75] G.P. Vasvari, G. Dyckhoff, F. Kashfi, B. Lemke, J. Lohr, B.M. Helmke, V. Schirrmacher, P.K. Plinkert, P. Beckhove, C.C. Herold-Mende, Combination of thalidomide and cisplatin in an head and neck squamous cell carcinomas model results in an enhanced antiangiogenic activity in vitro and in vivo, Int. J. Cancer 121 (2007) 1697–1704.
[76] A. Altmann, M. Sauter, S. Roesch, W. Mier, R. Warta, J. Debus, G. Dyckhoff, C. Herold-Mende, U. Haberkorn, Identification of a novel ITGαvβ6-binding peptide using protein separation and phage display, Clin. Cancer Res. 23 (2017) 4170–4180.